(22)

An Axial Force Sensor For a Prosthetic Knee

by

Theresa V. Iuzzolino

Submitted to the Department of Electrical Engineering and Computer Science in partial fulfillment of the requirements for the degrees of Master of Engineering in Electrical Engineering and Computer Science, Bachelor of Science in Computer Science and Electrical Engineering, and Bachelor of Science in Mechanical Engineering

at the

MASSACHUSETTS INSTITUTE OF TECHNOLOGY

May 28, 1998
[June 1998]

Author .....
Department of Electrical Engineering and Computer Science
May 28, 1998

Certified by .....
Professor Gill Pratt
Department of Electrical Engineering and Computer Science
Thesis Supervisor

Accepted by .....
Frederic Morgenthaler
Chairman, Department Committee on Graduate Theses

An Axial Force Sensor For a Prosthetic Knee

by Theresa V. Iuzzolino

Submitted to the Department of Electrical Engineering and Computer Science In partial fulfillment of the requirements for the degrees of Master of Engineering in Electrical Engineering and Computer Science, Bachelor of Science in Computer Science and Electrical Engineering, and Bachelor of Science in Mechanical Engineering.

May 28, 1998

Abstract

One out of every thousand people in the United States has had a limb amputated, with more than 30% of the amputations removing the knee. The MIT Leg Laboratory, in collaboration with Flex-Foot, is working on an intelligent above-knee prosthesis, requiring a light, short, and accurate axial force sensor. This thesis investigates a design proposed by Cullen [3], using a pressure sensor inside of two capped, concentric cylinders between which is a layer of silicone. Experiments were performed with GE's RTV 664 silicone, and the Motorola MPX5700D and MPX5999D, EG&G Model 83, and ACSI Model 7000 pressure sensors, and the Interlink Force Resisting Sensors. The design worked with the Motorola and EG&G sensors, but not reliably with the Interlink FSRs. The sensor can be reduced to 2 inches in length without much loss in stiffness. Greater accuracy and an investigation into the choice of silicones is still needed.

Thesis Supervisor: Professor Gill Pratt
Title: Assistant Professor, Department of Electrical Engineering and Computer Science

Acknowledgments

This thesis is my final hurdle to graduating and leaving MIT! In my nine years here (including time off), I've made a number of friends who have supported me throughout the years, and especially this last semester as I finished up all the work I had put off until the last moment.

I am especially grateful to Gill Pratt for giving me a chance to start a new thesis when my old one wasn't going anywhere, and for being patient with me when the work didn't go as fast as needed because I was working on US First and my classes.

I want to thank the people in the Leg Laboratory for all of their suggestions and pointers and for answering my questions even if the answer was "we haven't figured that out yet." These people are Gill Pratt, Olaf Bleck, Hugh Herr, Dan Paluska, Ari Wilkenfeld, Jerry Pratt, Mike Wittig, and Bruce Deffenbaugh.

A special thank you to Brian Gearing, a Mechanical Engineering graduate student who, without knowing me, generously offered to spend a couple of hours running tests on the sensors on an Instron machine for me.

I'm grateful to those people who have been patient with me, to my parents who probably wondered if I'd ever leave MIT, to Karen Sollins, my advisor, who cheerfully urged me on to completing my degrees and was never disappointed when I hadn't done as much as I said I would, and to Anne Hunter who has always given good advice and cares so much about all of the students and works hard to make sure we all graduate.

A big thank you to Nick Matsakis for helping me throughout this year, especially in these last weeks through his support and encouragement, through lessening my load by doing some of my day to day chores, and for bringing me meals during the last two weeks of my thesis. While others were living on pizza and takeout, I was dining on gourmet cuisine.

And thanks to Danilo too, who, in the last hours, saved me a lot of time by providing the paperwork and materials I needed to finish up the thesis.

I want to especially thank everyone who stood with me through this time in prayer: Brother Nick Austriaco, Nick Matsakis, Durodami, Danilo, Andrew and Wendy, Betty, Luis, and all those in Maranatha and CF who prayed for me. By God's grace this thesis is finished, and by His grace I was able to remain cheerful until the end.

Table of contents

Abstract 2

Acknowledgments 3

Table of contents 4

List of Figures 5

Chapter 1: Introduction 6

Chapter 2: Background 7

Chapter 3: Objectives 12

- Axial force sensor requirements 12
- Proposal for new sensor design 14
- Scope of analysis, design, and testing 17

Chapter 4: Axial Force Sensor Design 18

- Physical Design 18
- Analysis 19
- Discussion of analysis 26

Chapter 5: Prototype Design and Testing 29

- First stage of testing 29
- Second stage of testing 31
- Results 33

Chapter 6: Concluding Remarks 43

- Discussion 43
- Conclusions and Recommendations for Future Investigation 44

Bibliography 45

Data Sheets and Suppliers 46

Appendix A: Motorola Data Sheets 47

Appendix B: Honeywell Data Sheets 53

Appendix C: EG&G Model 83 Data Sheets 57

Appendix D: ACSI Sensor Data Sheets and Amplifier circuit diagrams from Model 7000 application notes 59

Appendix E: Interlink Electronics FSR Data Sheets 63

Appendix F: Pro-Engineer drawings 68

List of Figures

Figure 1: Walking cycle 8
Figure 2: Axial force sensor designed by Cullen 10
Figure 3: Axial force sensor modified by Goldfarb 11
Figure 4: Prosthesis assembly 12
Figure 5: Basic load cell design 15
Figure 6: Sensor designs 20
Figure 7: Diagram for theoretical analysis 21
Figure 8: Thin ring of silicone and effects of displacement by x_d 22
Figure 9: Shear triangle 22
Figure 10: Top layer of silicone 24
Figure 11: Cross-section of optimized inner cylinder 27
Figure 12: First stage testing sensors 29
Figure 13: Mold-making stand 30
Figure 14: Stage two test sensors 31
Figure 15: Motorola MPX5999D, 2" wall height, sensor output versus force 36
Figure 16: Motorola MPX5700D, 1" wall height, sensor output versus force 37
Figure 17: Motorola MPX5700D, 2" wall height, sensor output versus force 38
Figure 18: Motorola MPX5700D, 3" wall height, sensor output versus force 39
Figure 19: EG&G Model 83, 2" wall height, sensor output versus force 40
Figure 20: Single cycle of the Motorola MPX5999D sensor 41
Figure 21: Force versus displacement curves for 1", 2", and 3" stage two sensors 42

Chapter 1: Introduction

One out of every thousand people in the United States has had a limb amputated. Many of these amputations occur in the elderly where the effects of vascular disease require removing part of the leg or foot. In order to walk again, amputees use a mechanical prosthesis to substitute for the missing portion of the limb. The human body is designed to minimize the movement of the center of mass during walking, but a simple prosthesis is unable to fully the replace the functionality of the missing limb, causing an unnatural gait and a higher energy expenditure.

The MIT Leg Laboratory, with support from Flex-Foot Inc., is developing an intelligent prosthetic knee which will enable above-knee amputees (missing the foot, ankle, and knee) to have a more natural gait. The intelligent knee will determine how much torque to apply at the knee depending on how fast the person is walking and where they are in the stride cycle. To accomplish this, the control program needs to know how much weight the person is putting on the knee. The object of this thesis is to design an axial force sensor which will be placed below the electromechanical knee joint.

Chapter 2 is a brief overview of the stride cycle followed by a discussion of the types of prostheses on the market and the axial force sensors used in some of them. Chapter 3 discusses the objectives for the new axial force sensor, while chapter 4 gives a theoretical analysis of the basic sensor design and a discussion of the engineering trade-offs. Chapter 5 discusses the prototypes used for testing and the results. Chapter 6 concludes with recommendations for future research.

Chapter 2: Background

In the basic walking cycle each leg goes through two phases–the stance phase and the swing phase as shown in figure 1. In the stance phase, the leg is on the ground supporting the weight of the body, and in the swing phase, the foot is lifted off of the ground and the leg swings forward. The start of a step is marked by heel strike, when the heel hits the ground in front of the person. This is followed by toe-down where both the heel and the toe are touching the ground. The other leg then goes through toe-off which is the removal of the foot from the ground, and swings forward to start the next step with a heel strike.

Experiments show that the primary role of the knee in walking is to bend during the swing phase allowing the foot to lift off of the ground so that the body's center of mass changes as little as possible. The majority of the energy needed to walk comes from the hip, not the knee, and the knee acts primarily as a damper. It turns out that damping applied by the knee varies with the walking speed.

There are a variety of prosthetic knees currently on the market and being developed in labs. These range from a "peg leg" (no knee at all) to intelligent knees such as the Endolite Intelligent Prosthesis Plus, the Seattle Power Knee, and one being developed by the MIT Leg Laboratory. Since the knee acts primarily as a damper, many prosthetic knees are simply passive damping mechanisms. The damping coefficient is either preset or can be set manually by the user before, but not during, walking and determines the rate at which the amputee can naturally walk. Should the amputee choose to walk faster, the prosthetic leg will take too long for the heel to strike and the gait will be unnatural.

The object of the intelligent knee is to adjust the torque and damping coefficient applied by the knee in response to changes in the amputee's gait. The prosthesis needs to be able to adjust quickly to changes in the velocity of the user and unevenness in the terrain. The MIT Leg Laboratory is developing an intelligent knee based on research done by MIT Professor Woodie Flowers in the 1980s. The Flowers prosthesis is a programmable knee with a geared magnetic particle brake actuator and a SACH (solid ankle, cushioned heel) foot. A SACH foot has no joints in the ankle, but simulates the role of the

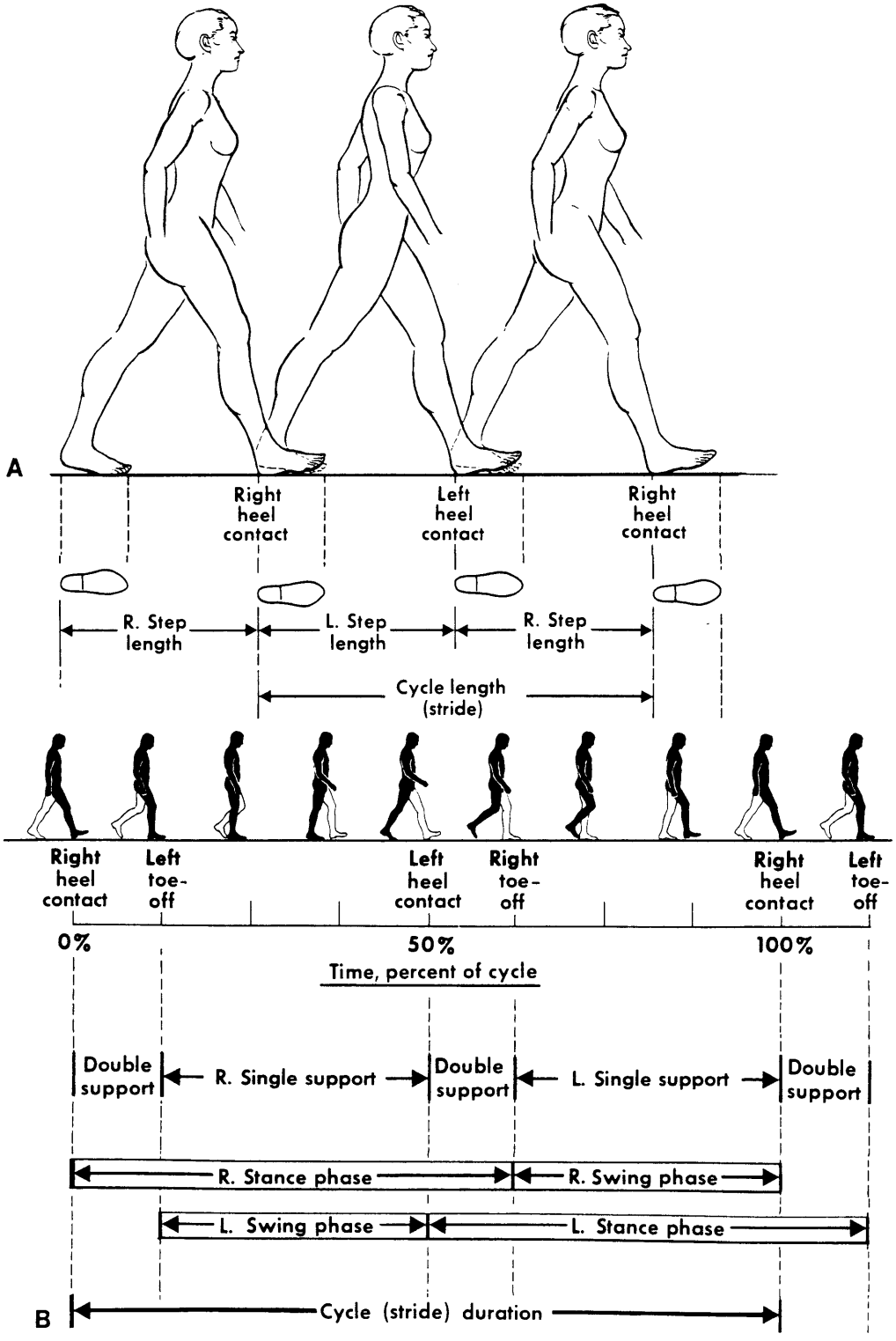

Figure 1: Walking cycle (from *Human Walking*, Inman et. al [6], page 26)

ankle's movement with a cushioned heel. The MIT Leg Laboratory, with funding from Flex-Foot, is designing a more powerful prosthesis with a direct drive magnetic particle brake and the next generation of control circuitry and software. The new design will be compact enough to allow Flex-Foot to add a flexible foot which allows rotation at the ankle joint. Because the flex-foot is taller and heavier than the SACH foot previously used, the prosthetic knee needs to be smaller and lighter than the Flowers knee. The new prosthesis will have a smaller actuator, electronics, and a shorter axial force sensor, which takes up 6 inches in the Flowers knee, nearly 1/3 of the length of the prosthesis.

The leg experiences significant bending moments during walking, yet the axial force sensor needs to measure only the force applied through the axis of the leg. The sensor must account for or get rid of the bending moment while being able to withstand it structurally. The axial force sensor on the Flowers knee was developed by Christopher Cullen [3] in 1984 and modified by Michael Goldfarb [4] in 1992. Cullen's design, as shown in figure 2, consists of two concentric cylinders with a silicone elastomer between them. The inner tube is capped, and a screw in the cap applies a force to a beam with a strain gauge.

In Goldfarb's design, shown in figure 3, the strain gauge is replaced by a linear magnetic potentiometer to get rid of frictional effects and to increase accuracy since the potentiometer has less drift. Despite this, the sensor still exhibits hysteresis and has been off by as much as 8 pounds at low forces. The purpose of this thesis is to use Cullen's basic design to develop a force sensor which is more reliable at low forces, smaller, cheaper, and lighter.

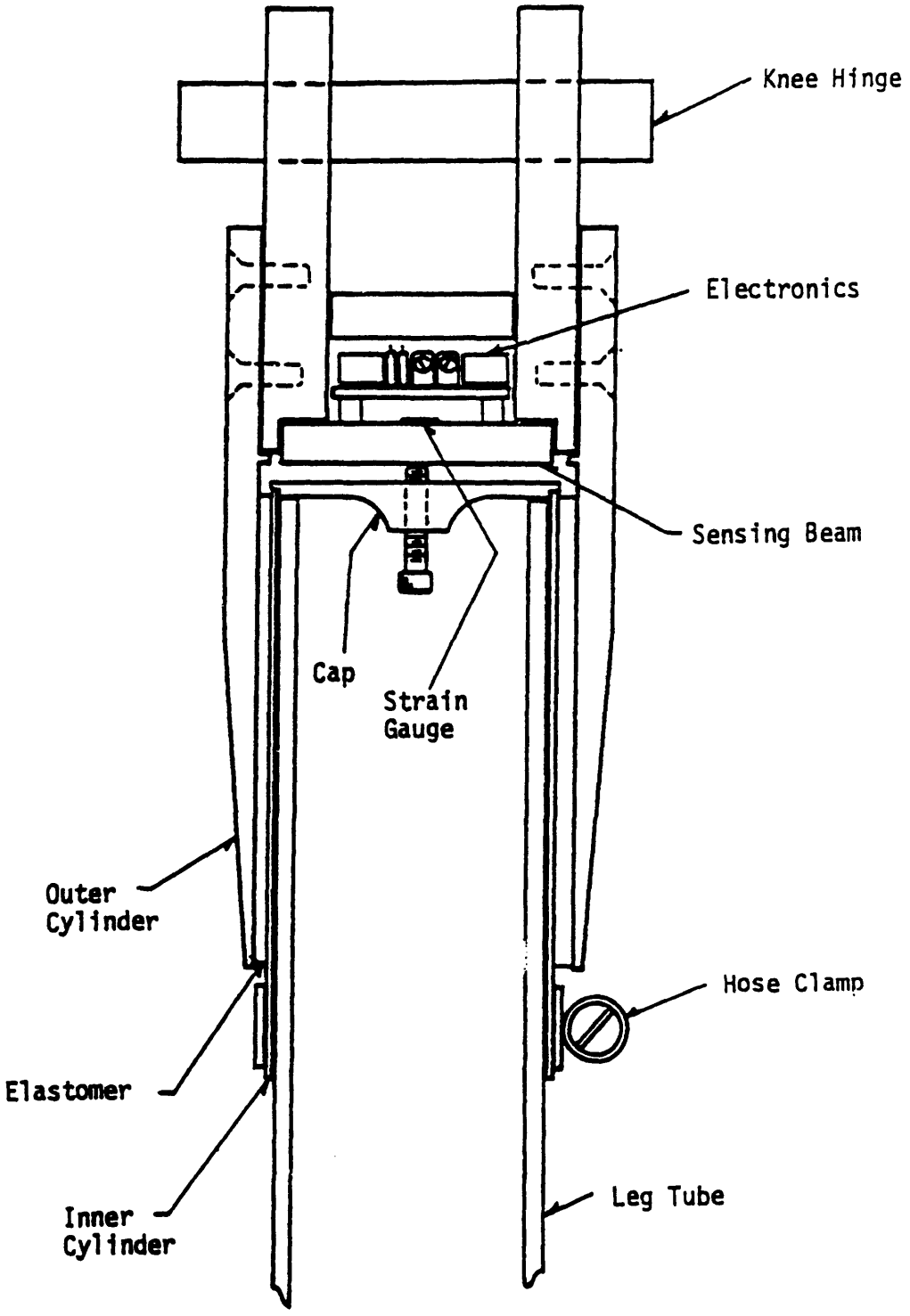

Figure 2: Axial force sensor designed by Cullen (taken from [3], pg 51)

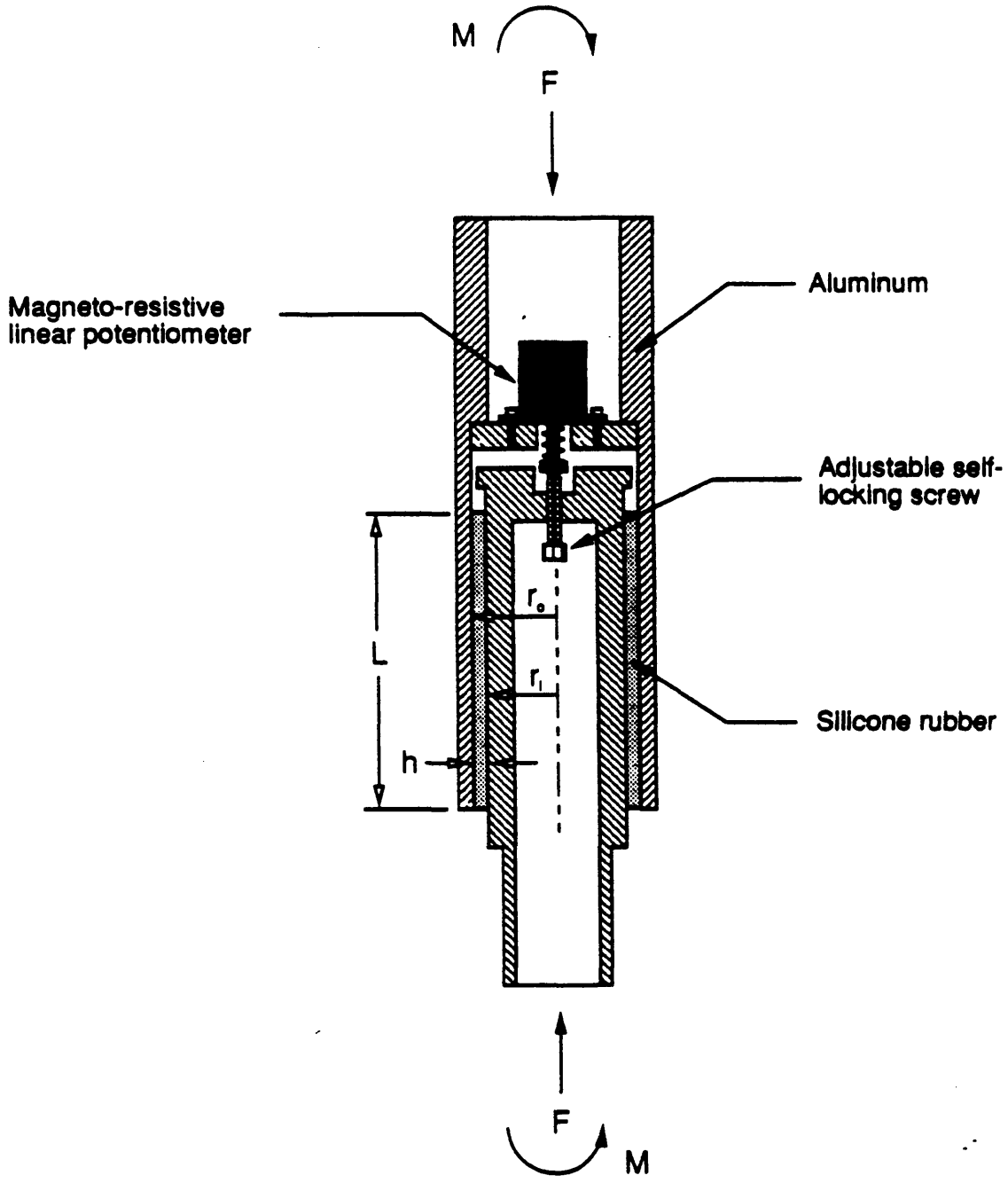

Figure 3: Axial force sensor modified by Goldfarb (taken from [4], pg 34)

Chapter 3: Objectives

Axial force sensor requirements

A prosthetic knee needs to be light, compact, strong, and inexpensive. The following requirements for the MIT Leg Laboratory's knee (not including the flex-foot) have been agreed on by Flex-Foot and the MIT Leg Laboratory. The knee must cost less than $750 to manufacture in quantities of 200 and weigh no more than 1 kg (2.2 pounds). It must be less than 30mm (1.2") from the top to the center of the knee, 200mm (7.9") from the center of the knee to the bottom, 60mm (2.36") in width (medial–lateral), and 70mm (2.75") in depth (anterior–posterior). The prosthesis must be able to support an average male (200+ lbs), and must therefore withstand very large forces and bending moments. The knee must have a lifetime of 3 years under moderate use, and the battery must support 10 hours of continuous use. Since the knee is targeted at a variety of users including people who are very active and who live in different climates, it needs to operate correctly over a range of temperatures, forces, and speeds.

The knee consists of a rotary magnetic brake filled with magnetic particle fluid whose viscosity changes with the strength of the magnetic field going through it. The larger the magnetic field, the higher the damping effect. The axial force sensor is attached below the knee, and the Flex-Foot is attached to the bottom of the sensor, as shown in figure 4. The electronics and batteries will be attached or placed inside of the knee brake or the sensor. Because the brake is magnetic, the axial force sensor must operate correctly near a magnetic field.

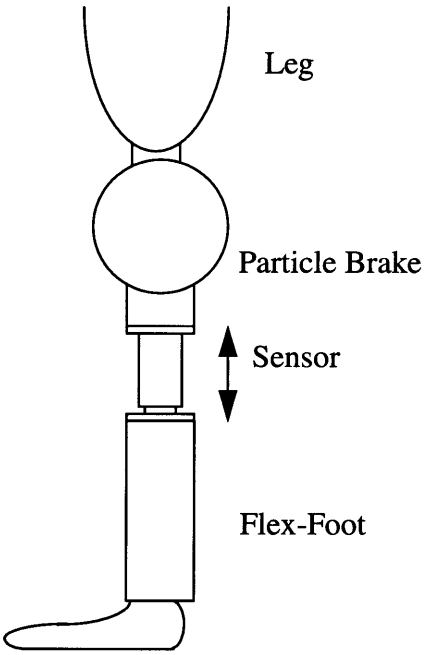

Figure 4: Prosthesis assembly

The size requirements for the axial force sensor are that it have a maximum height of 130mm (5.1") and be within the cross-sectional requirements for the knee, which were

60mm (2.36") medial-laterally and 70mm (2.75") anterior-posteriorly. The knee will be regularly subject to compression forces of 1120N (250lb) and moments around 80N-m [6, pg 102], but must be able to withstand forces of 3336N (750 pounds–three times body weight) and moments up to 120N-m [6, pg 95]. The knee needs to be able to withstand tensile forces around 120N[1]. The knee should be very stiff, with less than 6mm (1/4" of play) at the end of a 50cm (20") foot for moments experienced during walking [3, pg 63]. This is an angle of rotation of 0.72 degrees. Normal walking speeds range from 70 to 150 steps/min [6, pg 28], so a safe range of operation is 0 to 10Hz.

Ideally, the sensor should be temperature compensated giving constant readings over a range of -20 to 120 degrees Fahrenheit. It needs to be water resistant and have a high fatigue life, and must be light and inexpensive (under $100).

Until the controller development is finished and a more accurate sensor is placed on the knee, we can only estimate the accuracy requirements. To correctly respond to the gait of the user, the controller needs to know when the foot is on the ground, especially when heel-strike and toe-off occur, and to determine when the user is putting at least a third of his body weight on the leg. Heel-strike and toe-off occur at very low forces, around 1 or 2 pounds, accompanied by a moment around 20N-m [10, figures 3,5,6][6, pg 86], so the sensor should be accurate to within one pound in the 0 to 5 pound range. It should also be repeatable to within one pound for each cycle in this range so that the knee can operate consistently with each step, although drift over the lifetime of the sensor could be accounted for by the controller. It is desirable, but not necessary for the sensor to measure negative forces.

The sensor will be battery powered, with its output read by a microprocessor. It therefore needs to operate on a DC voltage under 12V, have an output range between 0 and 3V, and consume little power. The microprocessor will read the output of the sensor, and, if necessary, can use a lookup table to determine the correct conversion between voltage and force, so the sensor need not be linear. In fact, a non-linear sensor whose output varies

1. Estimate the force applied by a 5 kg mass with center of mass at 50cm (20") swinging at 5.2 rad/sec (150 steps/min, 120 degrees), using $F = ma = m\omega^2 r + mg$.

as the log of the force is desirable, because we need the same resolution between 1 and 10 pounds and 10 and 100 pounds.

Proposal for new sensor design

The difficulty in designing the axial force sensor is that the bending moment on the leg is very large and needs to either be measured and accounted for or prevented from reaching the force sensor.

One method of measuring the axial force is to use strain gauges to measure the strain in the metal in the leg. With gauges carefully placed at a equal distances on opposite sides of the axis of bending, the moment can be subtracted out. Strain gauges, however, require careful attachment, large amplifications, and they drift with time, although the latter could, as mentioned earlier, be compensated for in software.

Commercially available strain gauge-based load cells sell for $200-500. Those that are small and lightweight cannot withstand large bending moments. Those that can withstand the moments are generally bulky and heavy. Either way, they are too expensive for this knee.

In the Flowers knee, the axial force is determined using the displacement between two cylinders which have a 3 inch tall thin layer of silicone between them. This allows stress to be measured with a strain gauge sensing beam in Cullen's version and axial displacement to be measured in Goldfarb's version. The silicone between the cylinders opposes the moment applied to the sensor so that the strain gauge sensing beam is protected from the moment applied to the leg. In addition, silicone's modulus of elasticity is close to three times its shear modulus, which conveniently allows the desired axial movement while restricting bending.

The problem with Cullen's design is that there is a potential for frictional effects and wear due to the screw on the sensing beam. Goldfarb attempted to get rid of the friction using a linear magnetic potentiometer with a bias spring, but with movement, there is the problem of hysteresis. When energy is lost to heat in the loading cycle, the sensor does

not return to its original position. Voltages measured after the prosthesis is compressed and released differ from those taken after it is pulled and released, resulting in a reading that has been off by up to 8 pounds. The difference in these readings makes it difficult to determine when heel-strike and toe-off occur.

For this thesis, we use Cullen's basic design, but instead of using strain gauges glued to a beam, we measure the force on the leg by capping the top of both tubes and embedding a pressure or force sensor in a layer of silicone between them, as shown in figure 5.

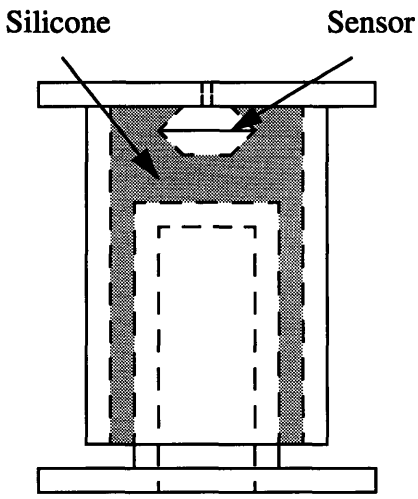

Figure 5: Axial force sensor design

Survey of sensors on the market

A survey of the pressure and force sensors on the market revealed a large number of expensive strain gauge based sensors, and a few other sensor technologies such as thick film, thin film, piezoresistive sensors, and force sensing resistors. We found four companies which manufacture pressure sensors which sell in small quantities for under $100: Motorola Semiconductor at $20, EG&G IC Sensors at $97, Honeywell/Micro Switch at $65, and Advanced Custom Sensors, Inc., for $45. We also experimented with force sensing resistors made by Interlink Electronics which are less than $10 each.

Motorola manufactures a series of semiconductor-based piezoresistive transducers where the piezoresistive material is laid on a small diaphragm that bends under pressure (see Appendix A for data sheets and diagrams). Piezoresistive materials change resistance under stress. The sensor has a chip housed in a silicon package with the back side of the chip exposed to air through a small vent, and the front side covered with a protective fluorosilicone gel. In order to use these sensors, the metal caps need to be removed and a small hole is placed in the top of the outer cylinder of the axial force sensor to leave the vent open to the air. We chose to experiment with Motorola's signal-conditioned, differential sensors with pressure limits of 1000KPa (150psi) for the MPX5999D and 700KPa

(100psi) for the MPX5700D. The signal-conditioned series is temperature compensated and calibrated, and the output has been amplified to give values between 0 and 5V. The differential chips measure gauge pressure. All of Motorola's pressure sensors are designed for air only since the fluorosilicone gel is water-permeable which could allow the thin leads from the chip to the pins to degrade. Attempts to use them in water have apparently been successful when the fluorosilicone gel was covered with another protective gel [18].

EG&G and Honeywell (Micro Switch division) also make piezoresistive semiconductor sensors. The Microswitch 40PC series has a cap with a port for attaching an air hose (see Appendix B for data sheets), and is similar to Motorola's pressure sensor with two small air holes in the back. Attempts to embed this chip in silicone failed because the chip is attached to the port, and taking off the port/metal cap tore the chip out as well.

EG&G IC Sensors makes a series of harsh environment sensors. The Model 83 is a closed metal container with the piezoresistive sensor in a liquid which transmits the force (see Appendix C for data sheets). The Model 83 is also temperature compensated using a ceramic chip with laser-trimmed resistors designed to compensate the output of each particular sensor. The sensor measures gauge pressure against a sealed cavity at atmospheric pressure.

Advanced Custom Sensors, Inc. (ACSI) sells strain gauge-based sensors, but uses a vacuum deposited thin film strain gauge instead of the traditional strain gauge attached by epoxy (see Appendix D for data sheets). The process allows them to make thinner strain gauge grid lines, and to sell their sensor for one fifth of the price of other strain gauge sensors. The Model 7000 is designed for use in hydraulic lines and is enclosed in a metal diaphragm. Like the EG&G Model 83, this model measures the pressure difference against a sealed atmospheric pressure reference cavity.

Another sensor with which we experimented is Interlink's Force Sensing Resistor (FSR). FSR's are thin plastic sensors with an interdigitating circuit printed on a plastic film and a second layer with a resistive substrate (see Appendix E for partial data sheets).

Under pressure, the films have a higher area of overlap which lowers the resistance. With these sensors, the log of the force varies inversely with the log of the resistance, a property that is perfect for our application. However, the sensors are only accurate to within 10%, and are not designed for precision measurements but are used as switches for touch control in electronic devices. We evaluated their use as an on-off switch to determine when heel-down and toe-off occur. These sensors come in a variety of sizes, all with the same force versus resistance curve. We used the small round sensors of sizes 0.2" and 0.5". The tail of the sensor must be exposed to atmospheric pressure since the sensor is measuring gauge pressure.

Scope of analysis, design, and testing

The development of the axial force sensor can be separated into two parts: design issues for a working sensor and manufacturing issues. We will look into some of the design issues, but not the manufacturing issues. Optimization of weight and space is a concern in design as well as manufacturing, and we will consider these in the design phase, but we will not attempt to find the optimal balance between cost, size, strength, useful life, and weight here. Temperature compensation is already done in most of the sensors and is a common technique so we will not address it, either.

The goal of the analysis is to understand the trade-offs in weight, size, strength and rigidity. The goal of the testing is to determine whether the overall design is suitable for our needs and how the sensors perform.

Chapter 4: Axial Force Sensor Design

Physical Design

Our design criteria are that the sensor be short, functional, lightweight, less than 2.3" in diameter, and have the prosthetics industry's standard four hole connector (four 1/4" holes on a circle of radius 2" at 90 degrees apart) on both the top and bottom of the sensor. The top of the sensor will be attached to the rotary knee actuator and may later be incorporated as one piece with the Flex-Foot will be attached to the bottom of the sensor.

Our goal is to transmit the axial force from the leg to the pressure or force sensor inside of the axial force sensor. Since the less expensive sensors cannot support the bending moment by themselves (and in some cases the weight either), the sensor must be embedded in a support structure. This structure acts like a spring in parallel, supporting part of the force along with the pressure sensor. If this support were a closed cylindrical container made out of aluminum or carbon fiber, a material rigid enough to withstand large bending moments would not transmit much of the force because it would act like a very strong spring in parallel. We therefore need a design that withstands large bending moments while transmitting large forces. This is the solution that Cullen proposed–the elastomer acts as a soft spring while the rigid cylinders support the bending moment. The pressure applied to the sensor is therefore proportional to the area of the tube as

$$P = \frac{F}{A} = \frac{F}{\pi r^2}.$$

The elastomer needs to have as low of a hysteresis as possible, and silicone is a logical choice. The silicone we chose was GE's mold-making RTV664. It has a durometer of 60 on the Shore A scale, and is a two part, platinum cure silicone which allows it to cure without exposure to air within 24 hours. A feature of the mold-making silicone is that it does not adhere to anything without a primer so as long as only the desired areas are painted with primer, the remainder of the silicone can be peeled away, allowing significant leeway in how the sensors are made.

We can fill the upper portion of the sensor with something other than silicone. If we use oil or water, there is a potential for leakage and it would make a mess if the sensor breaks. Furthermore, the Motorola sensors are not designed for either oil or water since the fluorosilicone is water permeable and water can damage the sensor. If the volume is filled with air, then temperature changes will change affect the pressure in the tube and change the reading. Since the material in the top needs to be soft enough transmit pressure evenly, an elastomer can be used. This elastomer does not need to be the same as the one on the sides.

Even though the pressure at a point should be the same in all directions, it makes the most sense to align the sensor so that the plane of the sensing surface is perpendicular to the axis of the force. Also, since there will still be some angular displacement, the sensor should be centered in the tube so that the pressure on the sensor has a minimal bending moment component. The sensor should be attached to one of the horizontal surfaces so that it doesn't move when the silicone is applied. Open gauge sensors such as the Motorola sensors will need an air hole as well. The EG&G sensor has a 9/16"-32 thread on it which allows it to be mounted through the wall. The electronics, however, come out of the back of the sensor, so it needs to be mounted through the inner cylinder, with a hole left for the wires to come out of the side. Sealed gauge pressure sensors can be completely enclosed with the wires coming out of the side of the outer cylinder.

We now have our basic design as shown in figure 6, and will proceed to analyze the effects of the geometry on the angular displacement, vertical displacement, strength, and weight.

Analysis

In the analysis that follows, refer to the picture in figure 7. R is the outer diameter of the layer of silicone on the side, and r is the inner diameter of the silicone. The thickness of this layer is sometimes referred to as t where $t = R - r$. The height of the thin silicone wall between the cylinders is L. The thickness of the silicone plug on top is h and is assumed to be solid silicone (no sensor present). The thickness of the aluminum tubing is a, and is assumed to be the same for both tubes. The moment, M, is applied along the y-

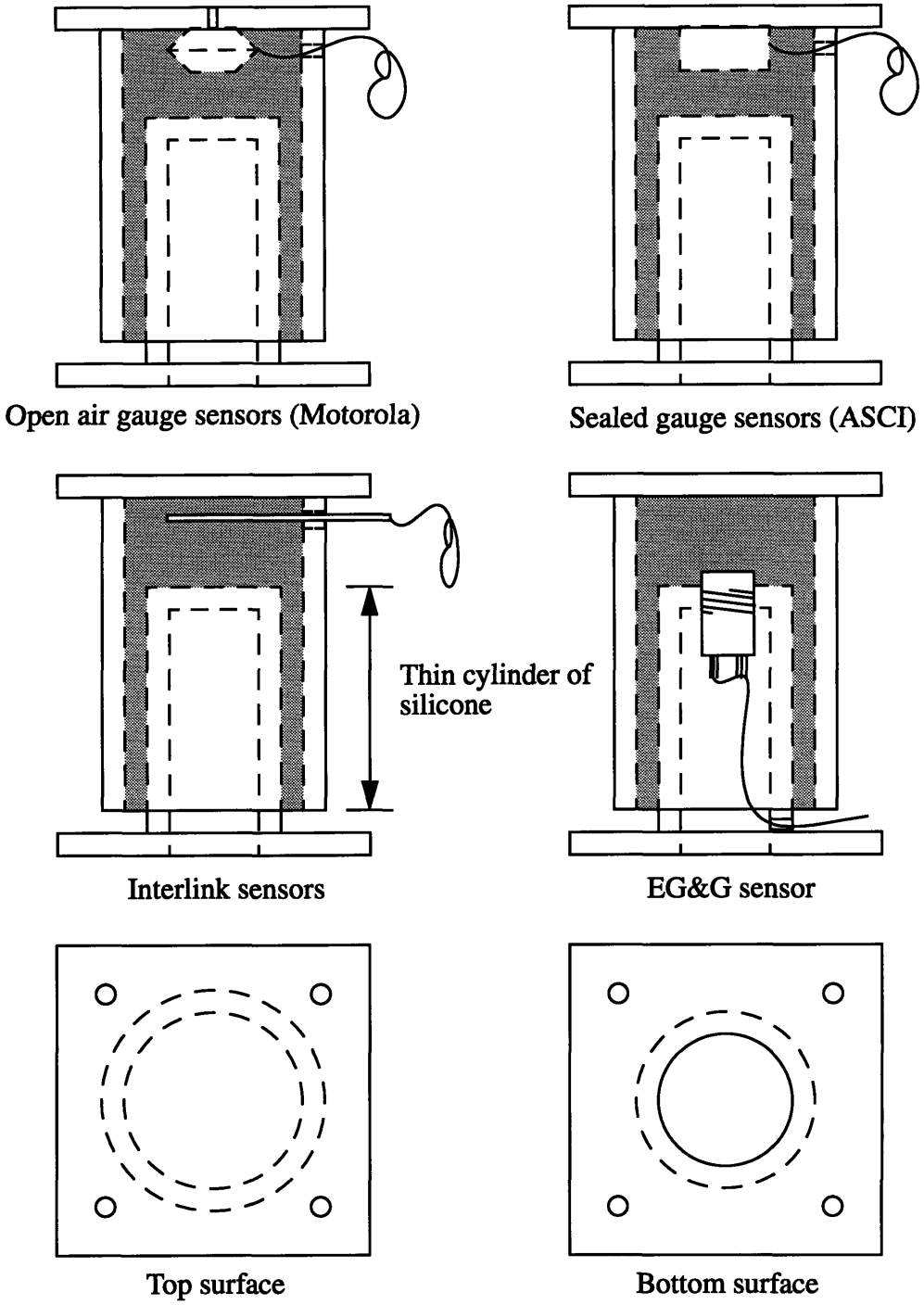

Figure 6: Sensor designs

axis and the force F along the z-axis. The angle of rotation, Θ, is assumed to be about the origin which is at the center of the thin cylinder of silicone. The modulus of elasticity is E, and the shear modulus is G. The thickness of the top and bottom square plates is P, with W

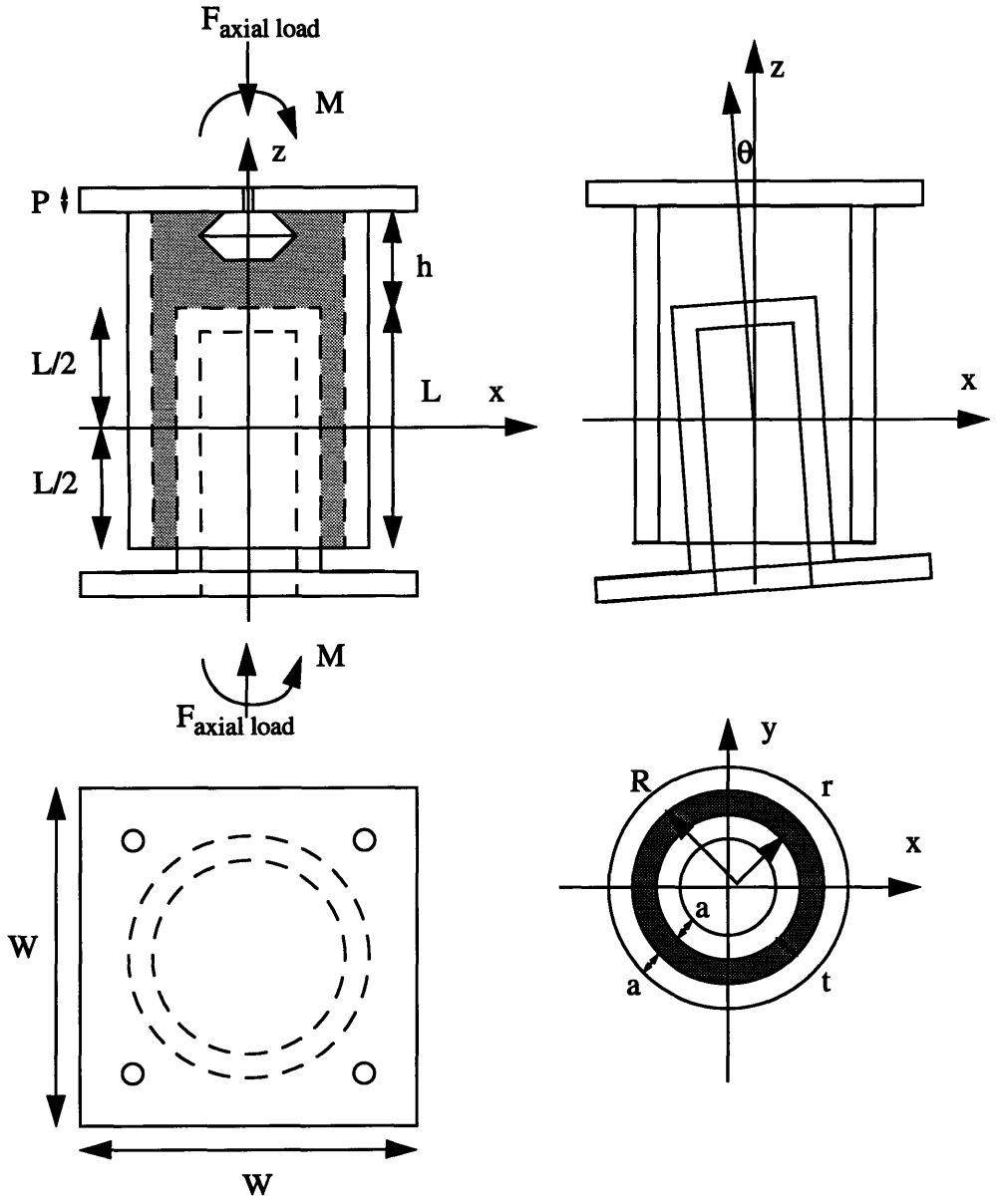

Figure 7: Diagram for theoretical analysis

as the width of each edge.

Bending moment versus angle

We will first analyze how the bending moment affects the angle of rotation. We can assume that the silicone is incompressible,[1] and therefore has constant volume. We will also assume that the silicone has a linear elastic region although this is almost certainly not

1. According to the GE Technical assistance.

true for high bending moments.

First, find the force applied by a thin ring of silicone of thickness, T, at a distance, z, from the origin, as shown in figure 8. Now analyze a small portion of the ring, where the uncompressed block is shown with a dashed line and the stress and shear produced by the horizontal displacement, $x_d = z\tan\theta$, are shown with the solid line. The force due to compression, F_{stress}, and the force due to shear, F_{shear}, both contribute to the force applied in the x-direction by the silicone such that

$$dF = dF_{shear}\cos\beta + dF_{stress}\sin\beta.$$

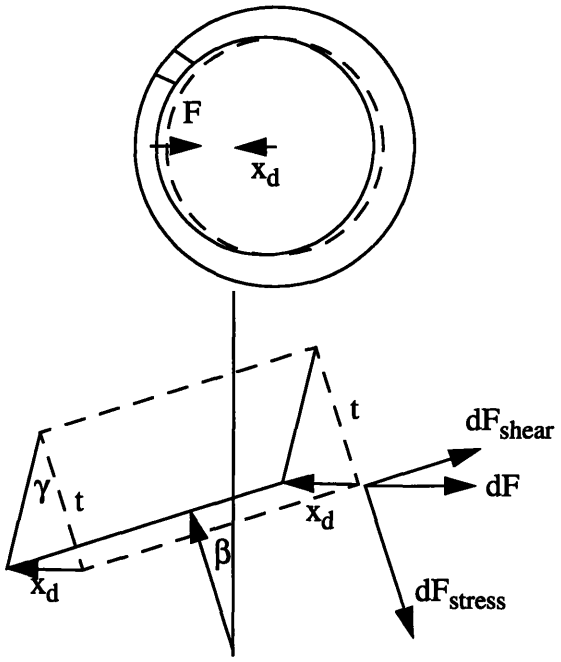

Figure 8: Thin ring of silicone and effects of displacement by x_d

The force due to stress is the stress times the area, $dF_{stress} = \sigma dA$, where the area is $A = Trd\beta$. The stress is related to the strain as $\sigma = E\varepsilon$, and the strain is the ratio of displacement and the original length, $\varepsilon = \frac{x_d\sin\beta}{t}$. This gives us a stress force of

$$dF_{stress} = \frac{ErTx_d\sin\beta d\beta}{t}.$$

The force due to shear is the shear times the area, $F_{shear} = \tau A$, where the shear is $\tau = G\gamma$. To calculate γ, we use two sides of the triangle, x_d and t, and the angle between these two sides, $90 - \beta$, as shown in figure 9. The third side is

$$s\sqrt{t^2 + x_d^2 - 2tx_d\sin\beta} =$$

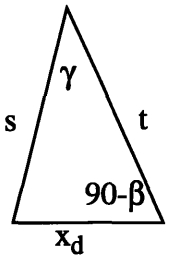

Figure 9: Shear triangle

using the law of cosines. Using the law of sines,

$$\gamma = \operatorname{asin}\frac{x_d \cos\beta}{s} = \operatorname{asin}\frac{x_d \cos\beta}{\sqrt{t^2 + x_d^2 - 2tx_d \sin\beta}}$$

and

$$F_{shear} = \operatorname{asin}\frac{x_d \cos\beta}{\sqrt{t^2 + x_d^2 - 2tx_d \sin\beta}}(GrTd\beta) \ .$$

This gives us a total force in the x-direction applied by a segment of the silicone as

$$\begin{aligned} dF &= dF_{stress}\sin\beta + dF_{shear}\cos\beta \\ &= \frac{ErTx_d \sin^2\beta d\beta}{t} + \operatorname{asin}\left(\frac{x_d \cos\beta}{\sqrt{t^2 + x_d^2 - 2tx_d \sin\beta}}\right)(GrT\cos\beta d\beta). \end{aligned}$$

The force applied by the whole ring of silicone is the sum of the forces applied by each segment, where the forces in the y-direction cancel because each has an opposing force in another part of the ring. The force applied in the x-direction is then the integral

$$F = \int dF = \int\left(\frac{ErTx_d \sin^2\beta d\beta}{t} + \operatorname{asin}\left(\frac{x_d \cos\beta}{\sqrt{t^2 + x_d^2 - 2tx_d \sin\beta}}\right)(GrT\cos\beta d\beta)\right)$$

which is, needless to say, a rather daunting integral. If we drop the shear term, we can find the force due to the stress alone, which is an underestimate for the force applied by the ring and therefore an overestimate of the angle of deflection for a given moment, thereby giving us a safety margin.

Taking into account the symmetry in the four quadrants and substituting for x_d, the force due to the stress alone on a ring of height T, at distance z from the origin, is

$$F = 4\int_0^{\frac{\pi}{2}} \frac{ErTx_d \sin^2\beta d\beta}{t} = \frac{\pi ErTz\tan\theta}{t}.$$

The moment that the silicone applies to the inner cylinder for an angular displacement of θ is the sum of the moments applied by slices of elastomer where $T = dz$. We

know that

$$dM_{cyl} = Fzdz$$

and integrating gives us

$$M_{cyl} = \int dM_{cyl} = \int_{-\frac{L}{2}}^{\frac{L}{2}} Fzdz = \int_{-\frac{L}{2}}^{\frac{L}{2}} \frac{\pi Erz^2 \tan\theta}{t} dz = \frac{\pi ErL^3 \tan\theta}{12t}$$

This is the moment applied by the thin layer of silicone between the cylinders.

Next, calculate the moment applied by the top layer of silicone as shown in figure 10. The top layer has radius R, but the silicone which is attached to the wall of the outer cylinder will also serve to pull or push on the inner cylinder to return to the silicone's original shape, so we use R as the radius of the disk instead of r. The force applied by a small area of silicone is

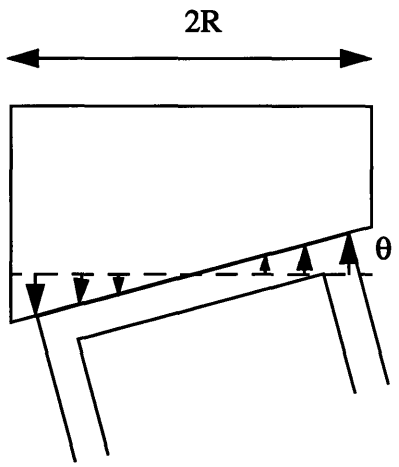

Figure 10: Top layer of silicone

$$dF = \sigma dA = E\varepsilon dA = \frac{Ez_d}{h} dA$$

where $z_d = x\tan\theta$ is the change in height of the elastomer. The moment is then

$$M_{top} = \int dF = \int_{Area} \frac{Ex^2 \tan\theta}{h} dA.$$

Using polar coordinates, and substituting for $x = r\cos\beta$ gives

$$M_{top} = 4\int_0^R \int_0^{\frac{\pi}{2}} \frac{Er^2 \cos^2\beta \tan\theta}{h} r dr d\beta = = \frac{\pi ER^4 \tan\theta}{4h}.$$

The sum of the two moments is then

$$M = M_{cyl} + M_{top} = \frac{\pi ErL^3 \tan\theta}{12t} + \frac{\pi ER^4 \tan\theta}{4h} = E\tan\theta\left(\frac{\pi rL^3}{12(R-r)} + \frac{\pi R^4}{4h}\right).$$

Structural yielding

The strength of the axial force sensor is affected mainly by the thickness and diame-

ter of the tubing, and the material it's made out of. Finding the yield strength of the tubing is straightforward if we assume no torsional loads.

For a structure subject to pure bending, the highest stress is at the point farthest from the neutral surface (the surface which experiences no force). In a cylinder, this surface passes through the axis, so the highest stress is experienced at the outer radius. The stress is related to the moment as

$$\sigma = \frac{-M_b y}{I_{zz}}$$

where M_b is the bending moment, y is the distance from the neutral axis, and I_{zz} is the moment of inertia along the z-axis [1, pg 256]. The moment of inertia for a cylinder is

$$I_{zz} = \pi(r_o^4 - r_i^4)$$

where r_o is the outer radius and r_i is the inner radius. The maximum stress is therefore in the z direction and is

$$\sigma = \frac{-M_b r_o}{\pi(r_o^4 - r_i^4)}.$$

Since the cross-sectional area of the tubing is constant, the force is uniformly distributed and the stress due to axial loading is uniformly distributed. The stress throughout the cylinder is therefore

$$\sigma = \frac{F}{A} = \frac{F}{\pi(r_o^2 - r_i^2)}$$

in the z-direction.

Since the compressive forces on the leg are considerably higher than the tensile forces, the maximum stress occurs when the material is in maximum compression. The maximum stress is therefore

$$\sigma_{max} = \frac{F}{\pi(r_o^2 - r_i^2)} + \frac{M_b r_o}{\pi(r_o^4 - r_i^4)}.$$

Mass

The mass is simply the sum of the masses of the tubes, the silicone, and the sensor. For simplicity, assume that the silicone fills the top of the tubes. Assuming the same thickness for both tubes, an overestimate for the mass of the tubes and their caps is

$$m_{tubes} \approx \rho_{tube}(2W^2P + 2\pi Lra + 2\pi(L+h)Ra).$$

The mass of the silicone is approximately

$$m_{silicone} \approx \rho_{silicone}(2\pi RtL + \pi R^2 h) \ .$$

The total mass for the axial force sensor is

$$m \approx \rho_{tube}(2W^2P + 2\pi Lra + 2\pi(L+h)Ra) + \rho_{silicone}(2\pi RtL + \pi R^2 h) + m_{sensor}$$

where m_{sensor} is the mass of the pressure sensor (this can be 0 for sensors which are lighter than the silicone they displaced). It is useful to note that the mass of the silicone increases as the square of the radius whereas the mass of the tubing increases roughly linearly with the wall thickness, the height, and the radius.

Discussion of analysis

Recall that we want the leg to rotate less than 0.72 degrees under loading over 60N-m. The analysis shows that one term in the bending moment increases as the cube of the length of the thin wall of elastomer, while the other term increases as the fourth power of the radius. It also shows that reducing the thickness of the silicone both in the side walls and in the top disk increases the resistance to the bending moment, although it turns out that the side-wall term is dominant. This makes sense intuitively since a thicker block of rubber is easier to compress than a thin one. The drawback to a smaller silicone wall size is that at a certain point, it is difficult to push a high viscosity liquid through a small hole.

As for strength, increasing the radius of the walls decreases the maximum stress by the square of the radius. The mass, on the other hand, increases linearly with the length, *L*, but as the square of the radius.

Table 1 gives theoretical values for the angle of deflection given different lengths, radii, etc., with M=80N-m, F=1120N, and E=2.6MPa and G=875kPa, the values for 60 Shore A durometer [8, pg 33-27]. From this table we can see that for the relative sizes for our sensor, the length has the most effect, followed by the thickness in the silicone side-wall, and then the radius. The thickness of the upper slab affects the degree of rotation by 3 thousandths of a degree, negligible for our purposes. This indicates that we should make the silicone slab around the pressure sensor as short as possible and use the space to add to the length of the side-wall instead. This poses a problem, however, since we need to keep enough silicone around the sensor to evenly distribute the pressure. One solution to this is to indent the inner tube as shown in figure 11 thus allowing us to increase the height of top slab of silicone without increasing the height of the sensor.

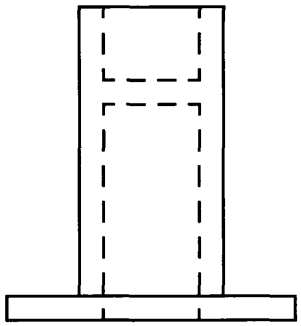

Figure 11: optimized inner cylinder

Another observation is that a radius of 2" versus 1.5" buys us very little in resistance to rotation, but increases the strength and the mass. If we use a material such as aluminum or carbon fiber, whose yield strengths can be over 80MPa [1, pg 108], the wall thickness needed to withstand a moment of 120N-m and a force of 1112N (250 pounds) for a radius of 2 inches is less than 0.005 inches. At that point buckling is a larger concern than the bending and axial forces. We can conclude, then, that increasing the radius is not necessary and increases our mass significantly.

With these guidelines in mind, we chose a design which has a silicone outer radius of R=1.425" and the wall thickness of the cylinders as appropriate for the material being used and the strength needed, although a thickness of 0.075 allows the standard sized leg post to fit inside of the inner cylinder. We experimented with different heights ranging from 1 to 3 inches and chose our thickness to be as low as possible at, t=0.025 inches, while still being able to make the sensors with a viscous silicone. The distance between the tops of the cylinders, h, is 0.5 inches. See Appendix F for CAD drawings.

Table 1: Dimensions and the angle of displacement (all lengths in inches)

	Outer radius, R	Thickness, t=R-r	Length, L	Top thickness, h	Angle (θ) in degrees
1	2.0000	0.0100	3.0000	0.2500	0.1519
2	2.0000	0.0100	3.0000	0.5000	0.1522
3	2.0000	0.0100	3.0000	0.7500	0.1523
4	1.5000	0.0100	3.0000	0.2500	0.2037
5	1.5000	0.0100	3.0000	0.5000	0.2039
6	1.5000	0.0100	3.0000	0.7500	0.2040
7	2.0000	0.0200	3.0000	0.2500	0.3054
8	2.0000	0.0200	3.0000	0.5000	0.3068
9	2.0000	0.0200	3.0000	0.7500	0.3073
10	1.0000	0.0100	3.0000	0.2500	0.3080
11	1.0000	0.0100	3.0000	0.5000	0.3081
12	1.0000	0.0100	3.0000	0.7500	0.3082
13	1.5000	0.0200	3.0000	0.2500	0.4122
14	1.5000	0.0200	3.0000	0.5000	0.4130
15	1.5000	0.0200	3.0000	0.7500	0.4132
16	2.0000	0.0300	3.0000	0.2500	0.4608
17	2.0000	0.0300	3.0000	0.5000	0.4639
18	2.0000	0.0300	3.0000	0.7500	0.4650
19	2.0000	0.0100	2.0000	0.2500	0.5072
20	2.0000	0.0100	2.0000	0.5000	0.5110
21	2.0000	0.0100	2.0000	0.7500	0.5123
22	1.5000	0.0300	3.0000	0.2500	0.6256
23	1.5000	0.0300	3.0000	0.5000	0.6274
24	1.5000	0.0300	3.0000	0.7500	0.6280
25	1.0000	0.0200	3.0000	0.2500	0.6285
26	1.0000	0.0200	3.0000	0.5000	0.6289
27	1.0000	0.0200	3.0000	0.7500	0.6290
28	1.5000	0.0100	2.0000	0.2500	0.6844
29	1.5000	0.0100	2.0000	0.5000	0.6866
30	1.5000	0.0100	2.0000	0.7500	0.6873
31	1.0000	0.0300	3.0000	0.2500	0.9622
32	1.0000	0.0300	3.0000	0.5000	0.9631
33	1.0000	0.0300	3.0000	0.7500	0.9634
34	2.0000	0.0200	2.0000	0.2500	1.0092
35	2.0000	0.0200	2.0000	0.5000	1.0245
36	2.0000	0.0200	2.0000	0.7500	1.0296
37	1.0000	0.0100	2.0000	0.2500	1.0382
38	1.0000	0.0100	2.0000	0.5000	1.0391
39	1.0000	0.0100	2.0000	0.7500	1.0395
40	1.5000	0.0200	2.0000	0.2500	1.3783
41	1.5000	0.0200	2.0000	0.5000	1.3872
42	1.5000	0.0200	2.0000	0.7500	1.3902
43	2.0000	0.0300	2.0000	0.2500	1.5062
44	2.0000	0.0300	2.0000	0.5000	1.5404
45	2.0000	0.0300	2.0000	0.7500	1.5521
46	1.5000	0.0300	2.0000	0.2500	2.0817

Chapter 5: Prototype Design and Testing

The testing for the prototype was done in two stages. In the first stage, we performed preliminary tests to confirm that the design would work, specifically that the pressure sensors can operate when covered with elastomer and that the output voltage changes when the sensors are compressed. The heights of the thin elastomer wall were varied to test the actual angle of rotation under bending. In the second stage, the pressure sensors were tested again with different heights and also with a different, more robust, design. The accuracy of these sensors was tested using an Instron machine.

First stage of testing

For the first round of tests, the axial force sensors were made so that the pressure sensors could be swapped between cylinders with different lengths of elastomer. Three cylinders were made with thin wall elastomer lengths of 2, 2.5, and 3 inches, and three sets of sensor plugs were made, one with a Motorola MPX5999D, one with an ACSI Model 7000 500 PSI, and one with a combination of the Interlink 0.2" sensor and Motorola MPX5999D. The axial force sensors fit together in three pieces as shown in figure 12: the hull with the two cylinders and elastomer, the plug with embedded sensor, and a cap which fits on top of the outer cylinder and keeps the sensor in place. The sensor plug fit into the top of the inner cylinder which was hollowed out to minimize the length of the entire sensor while maximizing the length of the elastomer wall. This design does not allow the sensors to be put in tension, but it does allows them to be preloaded by adding spacers under the sensor plug. The wires for the sensor come out the top through the cap.

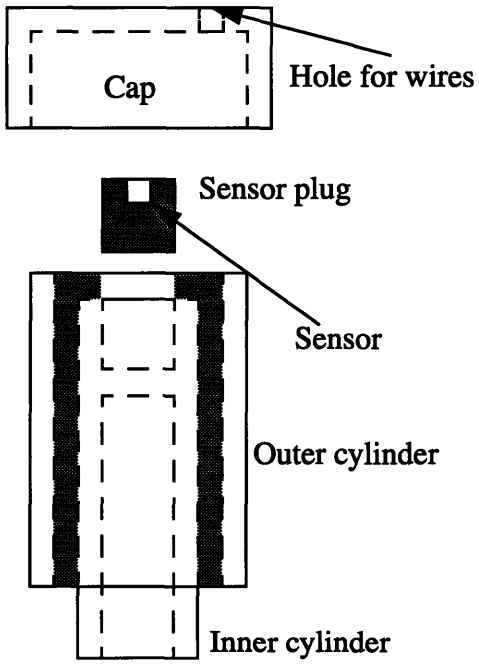

Figure 12: First stage testing sensors

To make the sensors, the inside of the outer cylinder and the outside of the inner cylinder were primed with GE Primer SS4155. Teflon spray was used on surfaces that were not supposed to have silicone. To keep the wall thickness even, the inner and outer cylinders were placed in a stand when curing as shown in figure 13. Three different methods were used to get the elastomer into between the cylinders. For the first cylinders, the viscous silicone liquid was spread on the inside of the outer cylinder, it was placed into the stand, and then the inner cylinder pressed into place. Although messy, it turned out to be the best method because the silicone filled all the crevices, and the extra silicone is easily peeled off of surfaces that have not been primed. The second cylinder was made by spreading the silicone on the inner cylinder, placing the outer cylinder into the stand, and forcing the inner cylinder into place. This resulted in a lack of silicone near bottom of the cylinders (top of the sensor) which had to be filled in later by filling up the stand with silicone and pressing the sensor back in, leaving air pockets in the sensor. The third sensor was made by placing the outer cylinder on the stand, leaving some silicone in the bottom of the outer cylinder, spreading the silicone on the outside of the inner cylinder and then pressing the inner cylinder into place. This method also has the potential of leaving air pockets.

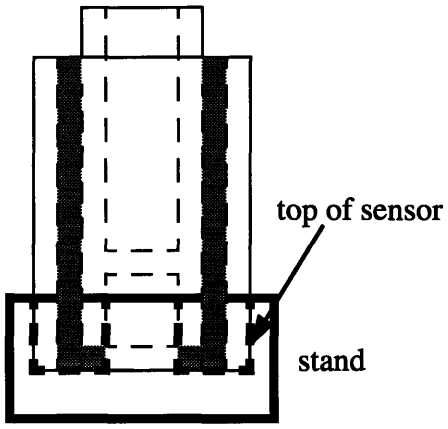

Figure 13: Mold-making stand

The sensor plugs were made by filling a cylindrical mold with silicone, putting the sensor into place, and then screwing on a cover plate (with a hole left for the sensor's wires) to make the top flat. This was successful for the ACSI sensor, but care had to be taken with the Motorola sensor to not get silicone in the back port. Double stick tape was used to hold the sensor on the top plate and lower it onto the silicone, but the tape didn't hold, the sensor was off center, and the thickness of the tape made the sensor surface lower than the plug surface. Normally, the silicone is supposed to be exposed to a vacuum of 26mmHg, but since this wasn't done air bubbles rose to the top of sensor plugs and stayed there since there was no means of escape.

First stage tests

Two tests were performed with the first stage sensors. For the first test, the deflection for a given moment was measured by placing weights at the end of an aluminum shaft attached to the inner cylinder. The outer cylinder was held in a vice, and the deflection of a point 21" from the lower edge of the outer cylinder was measured. Weights of 2.5, 5, and 10 pounds were hung at the end of the 0.5 inch aluminum shaft, 30.25 inches from the bottom of the outer cylinder. The deflection of the shaft alone was subtracted from the measured deflections giving the deflection due to the sensor alone. Sensors with thin wall lengths of 2, 2.5, and 3 inches were tested. While these tests were being performed, the voltage output of the Motorola sensors was monitored to see how the moment affects the sensor output. Repeated measurements were taken by loading and unloading with the weight.

The purpose of the second test was to observe how the voltage under an applied moment was affected by the Motorola pressure sensors being off-center. We measured the change in the voltage output for a given moment at different orientations of the cylinder. As before, the 10 pound weight was applied to the Motorola sensor in the 3 inch cylinder which was rotated along its axis to orientations of 0, 90, 180, and 270 degrees. Repeated measurements were taken by loading and unloading with the weight.

Second stage of testing

The second set of sensors were made from two capped aluminum cylinders as shown in figure 14. The inner cylinder was flat on top to simplify the machining, and had tapped holes in the side to adjust its placement before the silicone cures. Screws extending from the inner cylinder rest on the edge of the outer cylinder to keep the cylinders at the right distance, and to center the inner cylinder. Seven axial force sensors were made, as shown in table 2, with Motor-

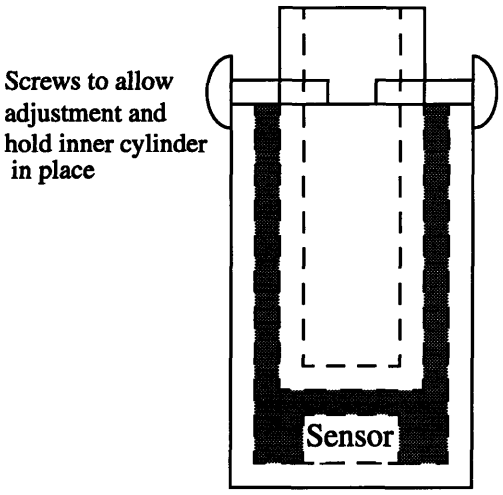

Figure 14: Stage two test sensors (upside-down)

Table 2: Second stage sensors

	Sensor type	elastomer height (inches)
1	Motorola MPX5700D	2
2	Motorola MPX5700D	3
3	EG&G Model 83	2
4	Motorola MPX5700D	1
5	Motorola MPX5999D	2
6	ACSI Model 7000, 300 PSI	2
7	Interlink FSR's, 0.2", 0.5"	2

ola MPX5700D sensors at elastomer wall heights of 1, 2, and 3 inches, and 2 inch wall heights for the Motorola MPX5999D, EG&G Model 83, and ASCI Model 7000, 300 PSI, pressure sensors and a sensor with two Interlink FSR's of diameters 0.2 and 0.5 inches. The wires for all sensors except the EG&G Model 83 came out of the side of the outer cylinder. The EG&G model had a half inch cylinder on top so that the force was applied to the cylinder, not the electronics.

The axial force sensors were made by gluing the pressure sensors to the top of the outer cylinder, filling the outer cylinder with silicone and then pressing the inner cylinder into place. The Motorola pressure sensors were attached with a ring of 5 minute epoxy around the bottom edge, held in place while it dried (with the metal cap loosened, but taped on) and centered using a pointed rod through the air hole in the top of the outer cylinder. The EG&G sensor was screwed into the top but not glued. The ACSI sensor was epoxied in place. Interlink sensors were allowed to hang freely in the outer cylinder, but were held in the correct orientation and distance by filling the hole for the wires with epoxy. All the wire holes for the other sensors were filled with epoxy as well.

All of the sensors were filled with silicone in the same way. First, the appropriate surfaces were primed, and the screws were adjusted so that the gap between the cylinders was even. After mixing the silicone, it was poured into the outer cylinder, and then placed in a makeshift vacuum chamber (using a vacuum cleaner). After 15 minutes, the inner

cylinders were forced down into the outer cylinders, causing the silicone to fill the thin wall and then pour over the sides. When enough of the silicone had been pressed out, the inner cylinder was fixed into place with the screws. While this method worked, it required a lot of force to push the inner cylinders down, and might be the cause of variation in the preloading of the sensors.

Second Stage Tests

Each of the seven sensors was tested using an Instron machine to determine how the voltage output varied with the force applied. The Instron machine was used with compression heads to apply a sine wave of frequency 0.01Hz and amplitude 448N (100lbs) centered around 448N giving an input force which varies from 0 to 996N (200 lbs). The data was sampled at 10Hz, and then averaged over one second intervals to produce one value per second. The data was averaged to counteract the noise added by the connection to the data acquisition card.

Table 3: Stage 1: Moment versus Angle of Rotation test
Displacement of sensor only (inches) and
Actual and theoretical angles of deflection (degrees)

	8.8N-m (2.5lb weight)			17.5N-m (5lb weight)			35N-m (10lb weight)		
Sensor	Disp.	Θ_{actual}	Θ_{theory}	Disp.	Θ_{actual}	Θ_{theory}	Disp.	Θ_{actual}	Θ_{theory}
2"	0.156	0.43	0.215	0.187	0.510	0.43	0.156	0.426	0.86
2.5"	0.0	0.0	0.184	0.0	0.0	0.26	0.094	0.256	0.42
3"	0.031	0.085	0.058	0.031	0.085	0.12	0.094	0.256	0.23

Results

Stage 1 Results

Table 3 shows the results of the moment versus angle of rotation test. Deflection values are given for the point which was 21" from the end minus the deflection of the rod of aluminum alone. These numbers are then turned into angles of rotation (Θ_{actual}). The theoretical values for the angle of rotation are included, and were calculated using the relations developed earlier.

For all of the sensors, the angles of deflection are within a factor of 2 of the theoret-

ical values although some are higher and some are lower. The displacement values for the 2.5" sensor were unexpected, but the wall thickness of the sensor is not actually uniform, and most likely the sensor was tested at an orientation where the inner cylinder was already at an angle, and no more deflection was possible. As we would expect, the 2 inch cylinder had a larger angle of deflection than the 3 inch cylinder, with the largest angle of deflection at 0.426 degrees for 35N-m on the 2 inch cylinder. Since the design requires at most a 0.72 degree of rotation at 80N, and since the rubber is not linear at high stresses, we may be able to get small enough rotations even at 80N-m. Because of this, we decided to experiment with thin wall heights around 2 inch for stage 2.

Table 4 shows the results of the moment versus output voltage test done with the 10 pound weight. This data is in line with our expectations. Since the 2.5 inch did not deflect much in the test, the voltage did not change much. For the 2 and 3 inch sensors, the voltage difference was higher for higher moments, and the 2inch sensor, which experienced a higher angle of rotation, also experienced a higher voltage change. The unloaded output is given in the results since the preloading was different for different lengths of tubing.

Table 4: Stage 1: Moment versus Motorola MPX5999D output

Sensor	2.5lb (mV)	5lb (mV)	10lb (mV)	Unloaded output (V)
3"	2	4	9	0.46
2.5"	-1	-1	1	0.57
2"	17	24	27	0.54 to 0.59

In order to understand the values from the previous experiment, we decided to see if the orientation of the axial force sensor under bending made a difference in the output of the pressure sensor. The results reported in table 5 show that this was the case. Close examination of the sensors while placed in the 2 and 3 inch cylinders, shows that the Motorola sensor is not centered (the center is assumed to be at the port based on the drawings in the Motorola data sheets). Regardless of where the sensor is, though, we expect that loading it at 0 degrees should give an equal and opposite value from loading it at 180 degrees if the pressure is not evenly distributed, and should give no change in value if the pressure is evenly distributed since there is no change in volume. Things are not quite this

simple, though, since the fluorosilicone in the Motorola sensor is sticky and will change shape when the silicone moves. The values were opposites for everything except the 2 inch sensor for 0 and 180 degrees which were both the same sign and equally large. This is puzzling, but we can conclude that it is important to center the Motorola sensor so that the bending moment affects it as little as possible, and that a softer silicone gel in the cap may be necessary.

Table 5: Moment vs. Orientation of sensor (MPX5999D)

	Orientation			
Sensor	0^o (mV)	90^o (mV)	180^o (mV)	270^o (mV)
3"	-11	-15.8	0.3	19
2"	20.75	-3.2	18	-18

Stage 2 Results

The results of the Instron tests of force versus sensor output are shown in figures 15 through 19. (Results for the ACSI Model 7000, 300psi sensor were omitted because we were unable to get it sufficiently amplified during the test. Stage 1 experiments showed that it did work while embedded in silicone though.). Figures 15 through 18 show the Motorola MPX5700D and MPX5999D tests with thin wall lengths of 1, 2, and 3 inches for the Motorola MPX5700D and 2 inches for the MPX5999D. The force versus displacement curves are fairly linear except for an unexpected abnormality in sensor 1 (figure 17) and show a difference of 0.4V across 200 pounds, a sensitivity of 2mV/lb. Sensor 1 was most likely preloaded in tension. If the resistance is the same for values in tension or compression, then the dip is caused by going from tension to compression in the sensor.

The Motorola sensors show a distinct hysteresis. Figure 20 shows the output for one cycle of the force, and figures 15 through19 indicate output values during increasing force with 'o's and decreasing force with 'x's. As we can see, the falling edge tends to the upper side of the curve, and the rising edge to the lower.

When an Interlink sensor has no force applied, there is actually no resistance across it, but when contact is first made, the resistance drops to 2MΩ. Tests on Interlink sensors

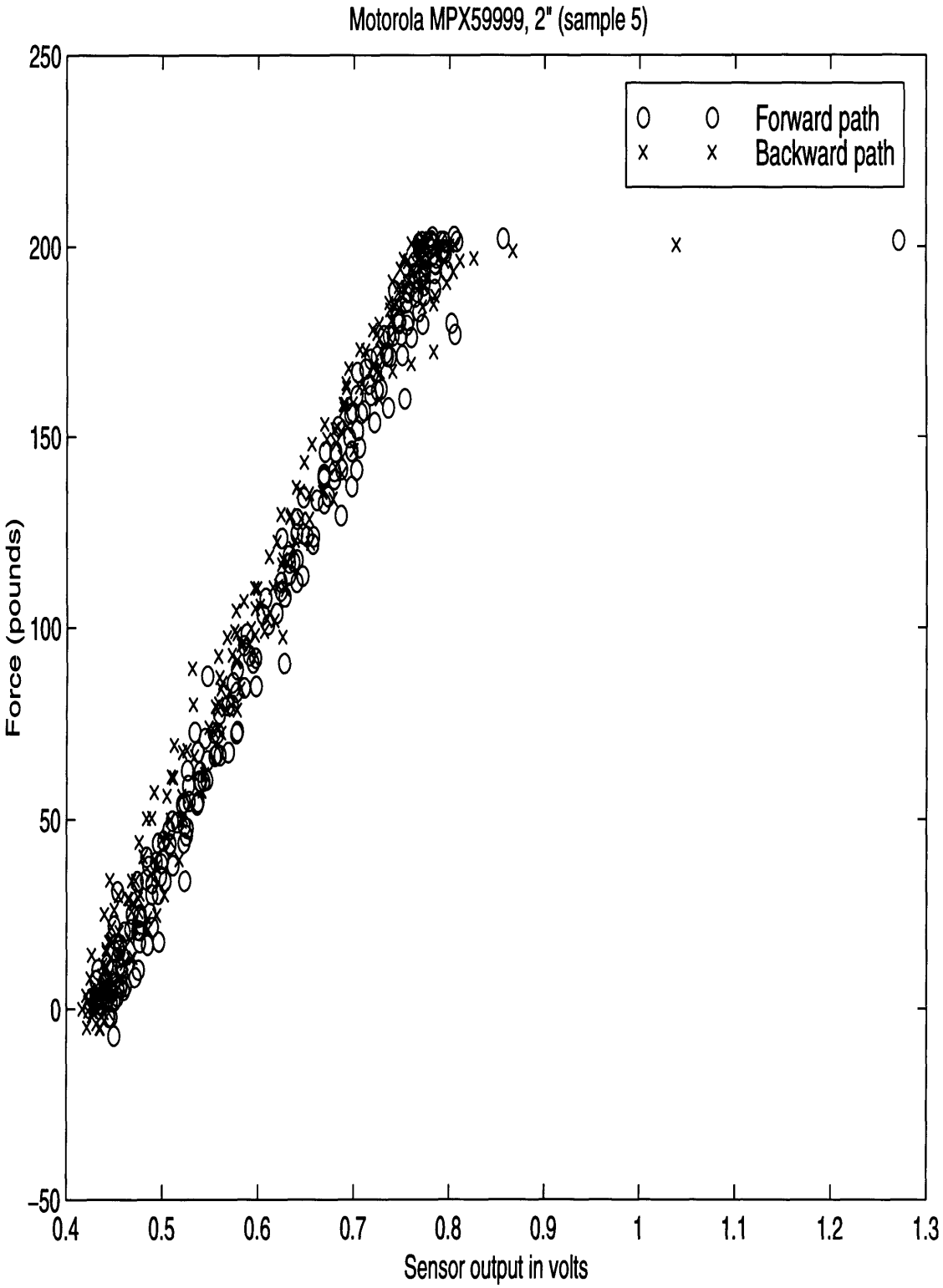

Figure 15: Motorola MPX5999D, 2" wall height, sensor output vs. force diagram

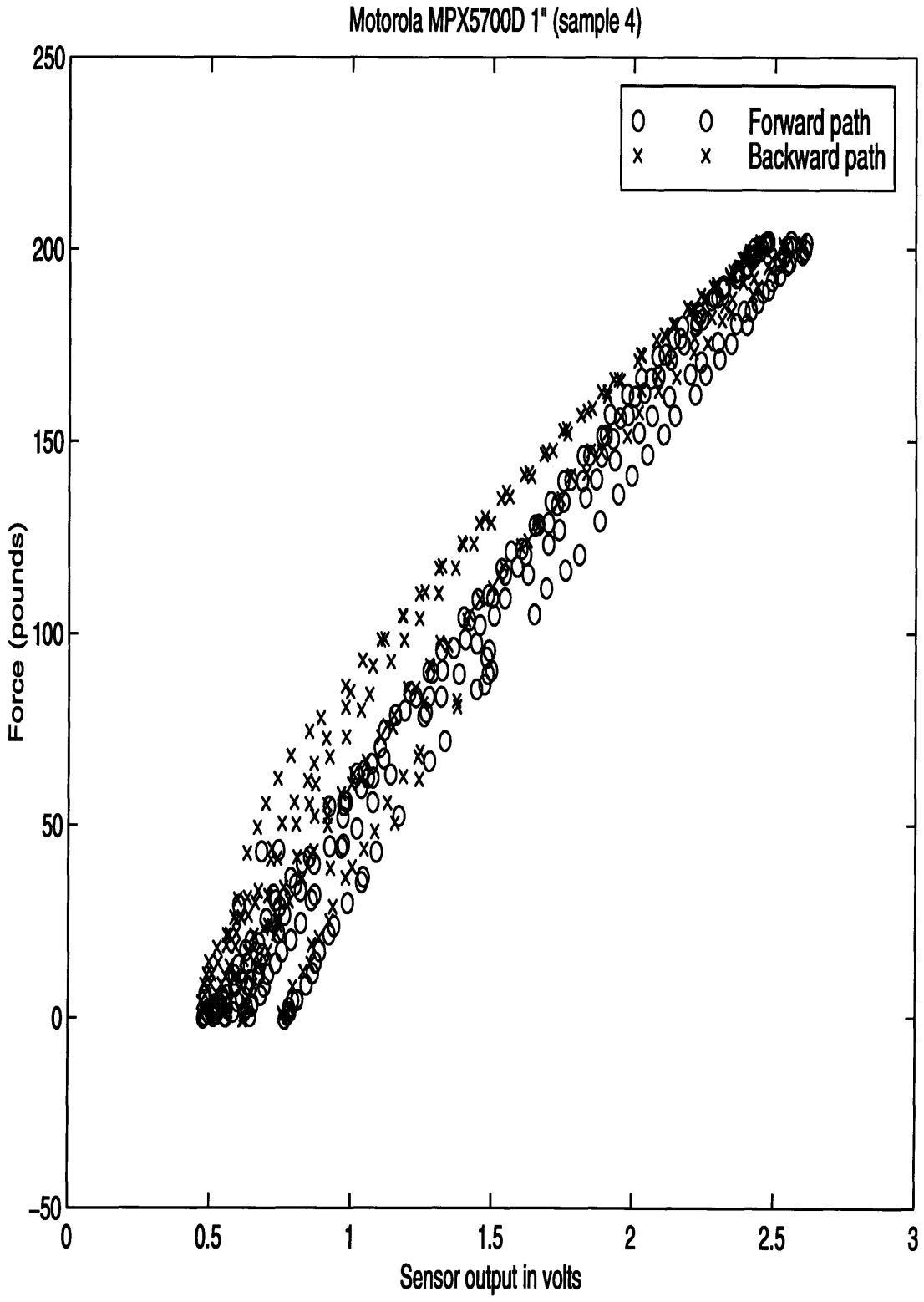

Figure 16: Motorola MPX5700D, 1" wall height, sensor output vs. force diagram

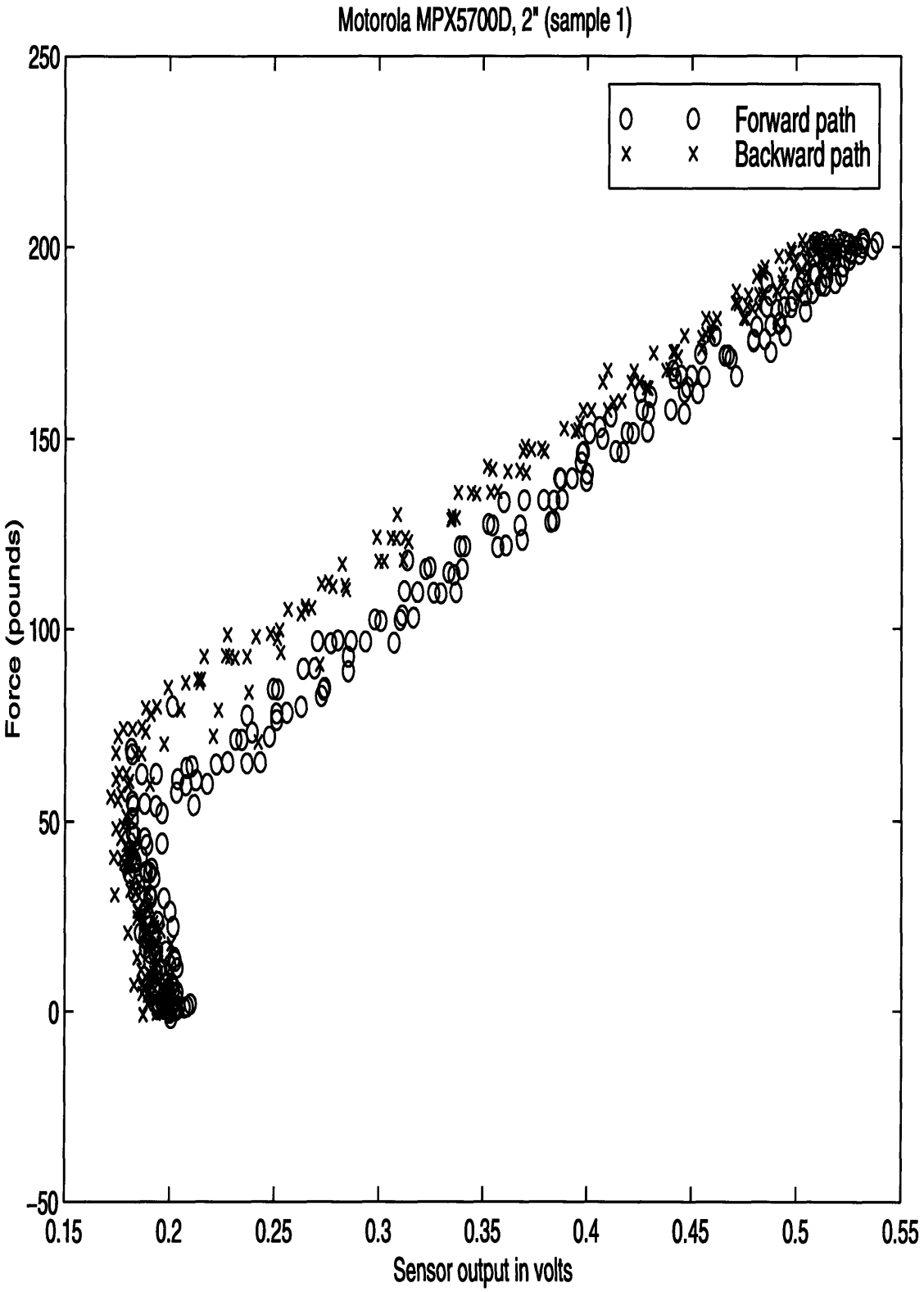

Figure 17: Motorola MPX5700D, 2" wall height, sensor output vs. force diagram

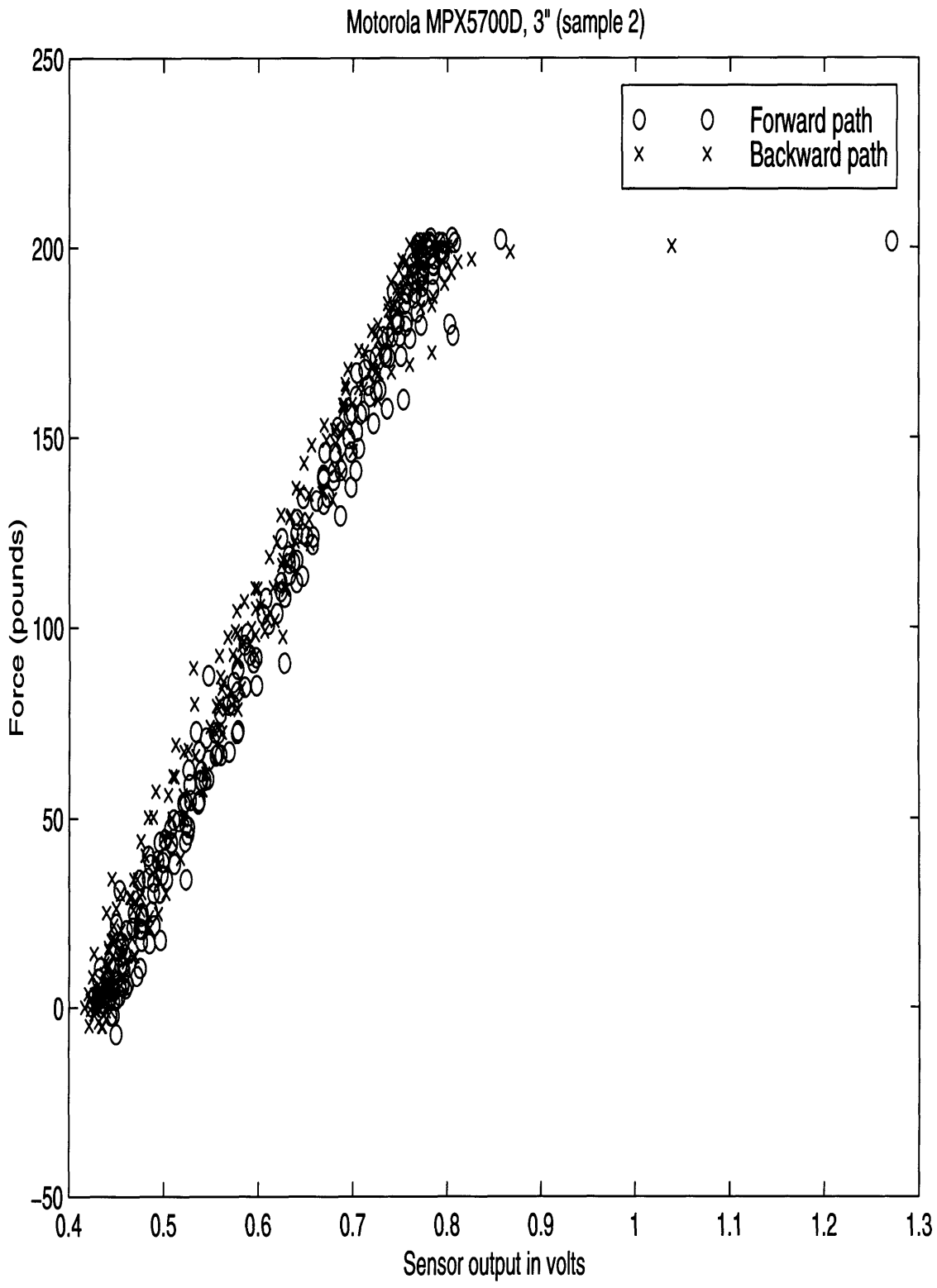

Figure 18: Motorola MPX5700D, 3" wall height, sensor output vs. force diagram

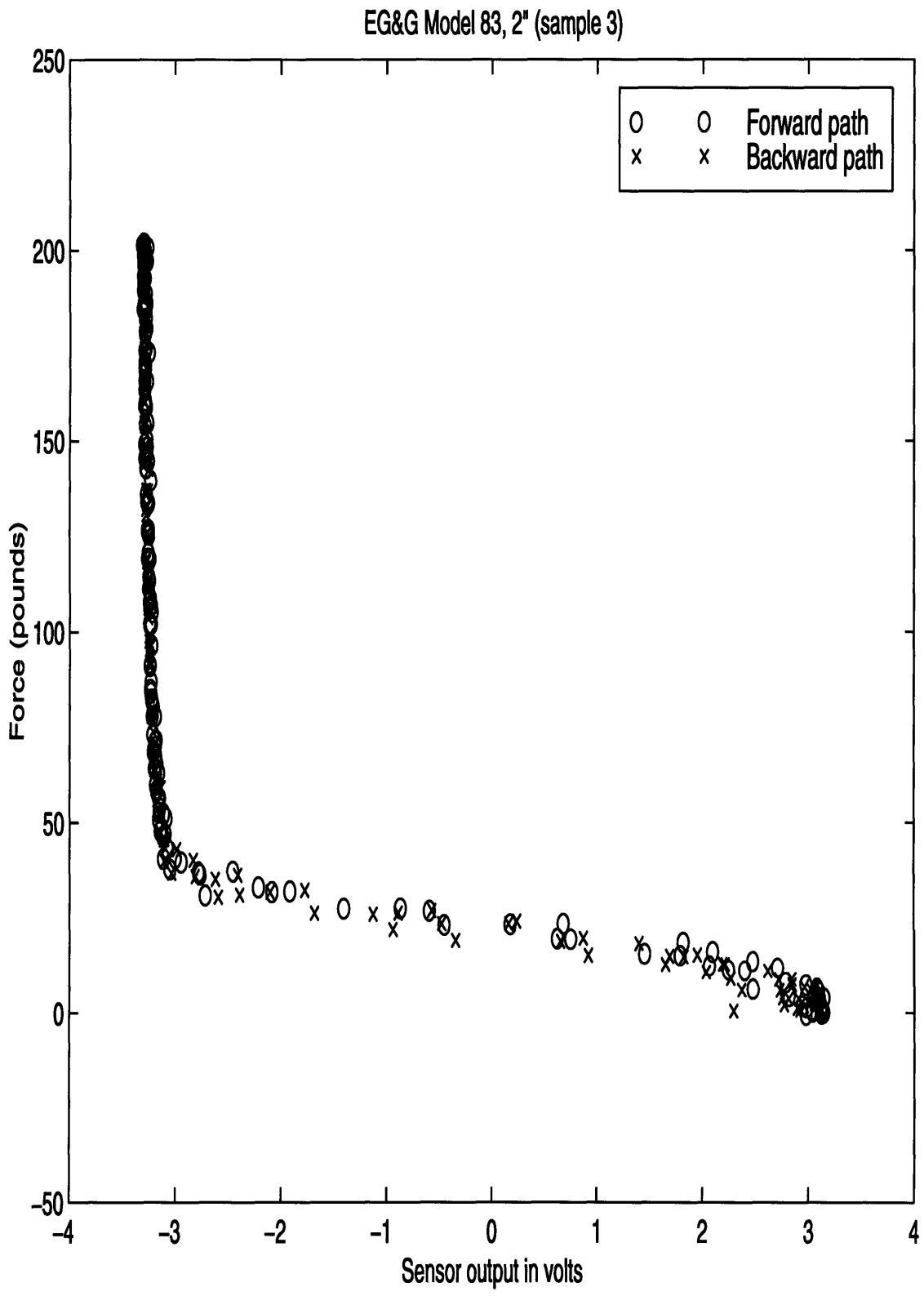

Figure 19: EG&G Model 83, 2" wall height, sensor output vs. force diagram

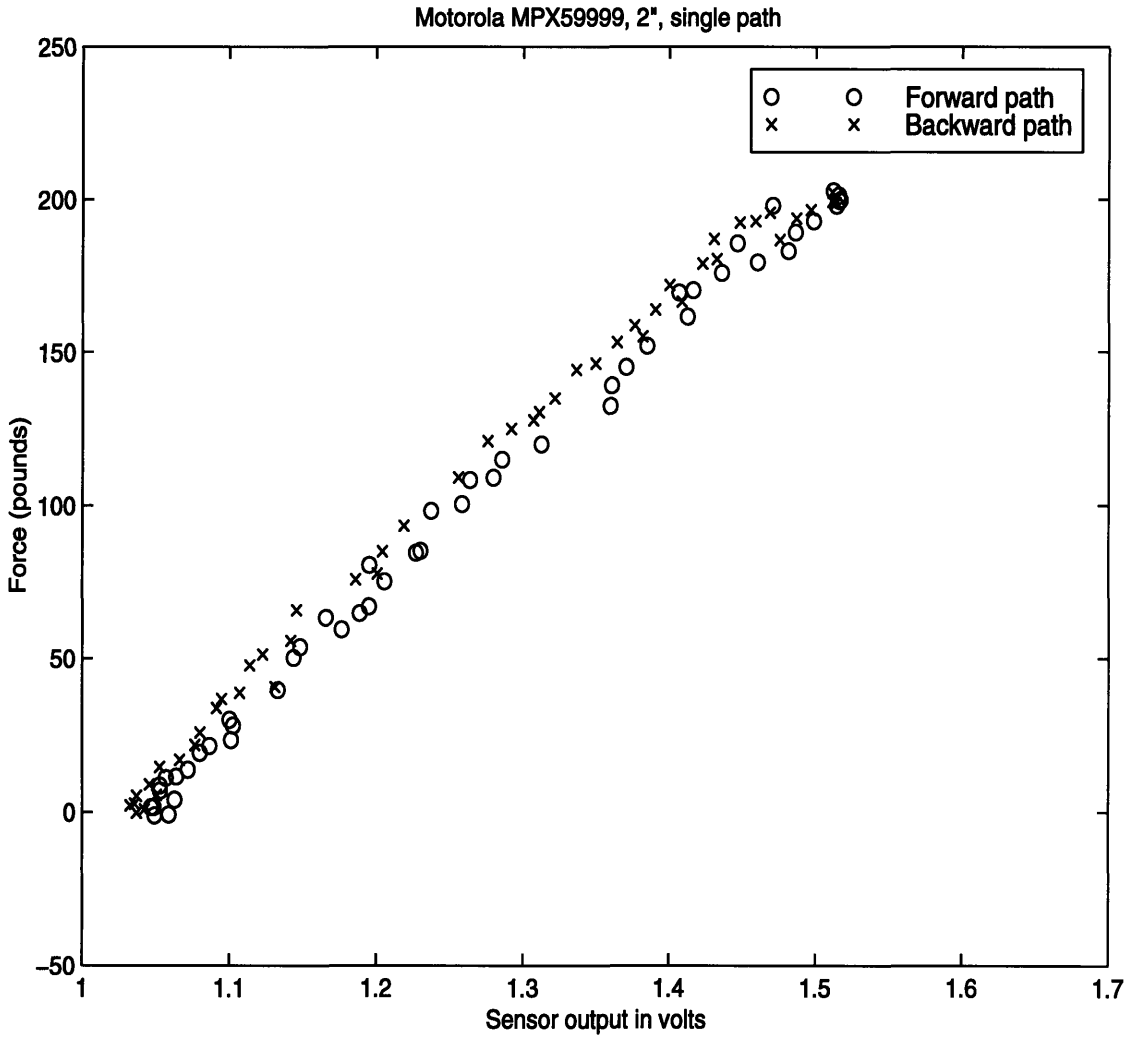

Figure 20: Single cycle of the Motorola MPX5999D sensor

in stage 1 and stage 2 axial force sensors showed that the Interlink sensors are not very sensitive when embedded in silicone. Sometimes the sensor would go off after significant (20 pounds or more) weight was put on the axial force sensor, and sometimes they wouldn't go off at all. In the stage 2 sensor, after a period of testing, one sensor was permanently off, and the other was permanently on.

The EG&G Model 83 sensor showed promising results. The force versus voltage curve, as shown in figure 19 shows no significant hysteresis, a thinner band of values, and high accuracy at low forces. The clustering of voltages at -3 and 3V is most likely due to amplification circuit since the EG&G sensor has an internal wheatstone bridge and the

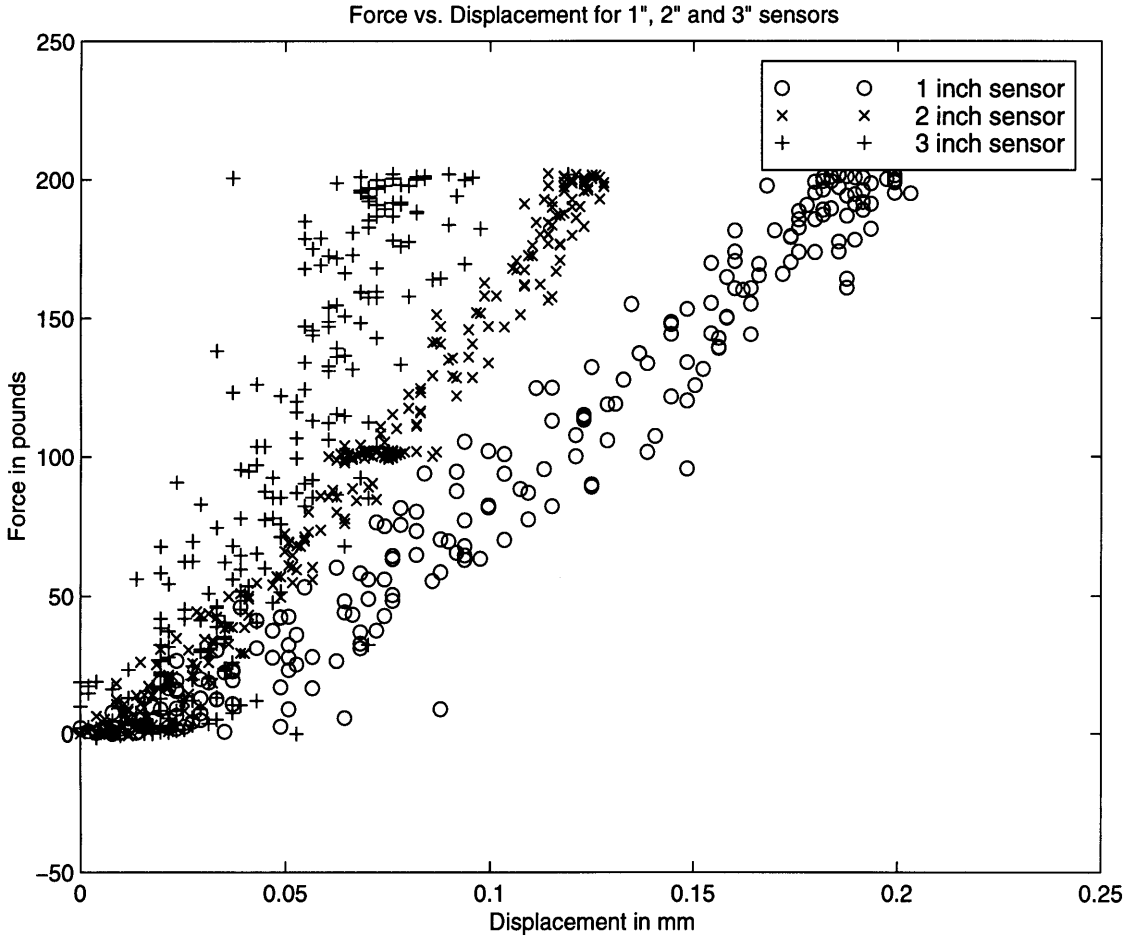

Figure 21: Force versus displacement curves for 1", 2" and 3" stage two sensors

output can be amplified as needed. The EG&G sensor is rated up to 300psi, so its full range is much greater than we would have reached with 200 pounds of force applied across a 1.5 inch diameter circle.

The Instron machine is able to measure the displacement of a sample, so we include here force versus displacement curves for the stage 2 sensors of heights 1, 2, and 3 inches (axial loading only) in figure 21. The results followed our expectations, with the 3 inch sensor displacing least. The strain, ε, is equal to the displacement, d, over the length, L, of the thin silicone wall, and

$$F = \sigma A = E\varepsilon A = E\frac{d}{L}A$$

where F is the force, E is the Young's modulus, A is the area, and σ is the strain. This tells us that for a constant force, the displacement is proportional to the length.

Chapter 6: Concluding Remarks

Discussion

Overall, the tests were successful indicating that the design works in practice. The accuracy is dependent on the sensors, though, and may not be sufficient for our needs. The bending versus angle test indicates that we can make a short, yet stiff, sensor, however, the shorter the sensor, the more the moment affects the sensor output.

Some problems arose while running the tests. The first is that during stage 1, the Motorola sensor's value would occasionally drift at approximately 1mV/s. The drift would stop when the cap was tightened, but the fact that this drift happened under no load indicates that care needs to be taken in making sure that the cap doesn't move. The safest way of doing this is to make the top and side of the outer cylinder one piece, which reduces the weight as well. The fact that some of the Motorola sensors in stage 2 exhibited the same problem is strange. This problem needs further investigation.

The sensitivity of the Motorola pressure sensors is much lower than expected. The expected pressure range for a silicone plug of diameter 1.425 inches undergoing loads up to 200 pounds is $P = \frac{F}{\pi r^2} = \frac{200\text{lb}}{\pi(0.713\text{in})^2} = 125\text{psi}$ or 865kPa. The actual range that the pressure sensors are seeing is 0.4V which is 8% of the range of the sensor, and a measurement of less than 12psi. One possible explanation is that the fluorosilicone gel is compressible and does not transmit the entire load. Another possibility is that the load is not evenly distributed throughout the silicone and that a lower durometer silicone should be used. A third possibility is that there were still air bubbles in the GE silicone causing it to become compressible, and that greater care needs to be taken to ensure that air bubbles are removed.

In all of the experiments, the sensors were newly made and had not be broken in. The outputs may be more reliable after cycling them for a while.

Conclusions and Recommendations for Future Investigation

In these experiments, we found that the basic design worked, but not entirely as we expected it to. The Motorola sensor readings drifted even when no force was applied, and also did not measure with the predicted sensitivity. Since the Motorola sensors are the least expensive ($20 for one, $16 or less in bulk), it would be worthwhile to solve the drifting problem. The low sensitivity can be remedied by buying a more sensitive version such as the MPX5100D which is rated for 14.5 PSI.

A closer look at the EG&G sensor would also be worthwhile to determine its accuracy at weights between 0 and 10 pounds, and to see if it is suitable for this application. The drawback to the EG&G sensor is that it is the most expensive one we tested at $97 for one and $74 for quantities over 499. Investigation into other sensors on the market should continue, as well as seeing if the ACSI sensor will work.

We chose silicone as the elastomer because silicones have low hysteresis, and there are RTV (room temperature vulcanizing) platinum cure silicones which we can easily use for our application. The platinum cures do not attach to anything without a primer making the molding process easier. Further investigation into the type and durometer of the silicone is needed. Experiments should be carried out with a low durometer silicone in the sensor area, and a high durometer silicone in the thin side wall. Experimenting with the silicones used in superballs would be worthwhile since the companies measure the hysteresis for only a few silicones, and it is possible it there may be a large variation. Also, investigation should continue into the appropriateness of other elastomers.

We did not do any fatigue or temperature testing, but such tests need to be carried out to guarantee that the sensor can weather the constant use. Also, tests need to be done with strong magnets to see if they affect the sensor.

The preliminary results show that this design for a sensor has promise and is worth further investigation. The mechanical properties are satisfactory since the sensor can be made short enough to fit into the prosthesis and strong enough to not deflect greatly. Further investigation towards improving the accuracy of the sensor is needed.

Bibliography

1. Ashby, M. F.
Materials Selection in Mechanical Design
Pergamon Press Ltd, Great Britain, 1995.

2. Crandall, Stephen H., Dahl, Norman C., Lardner, Thomas J., et. al.
An Introduction to The Mechanics of Solids, 2nd Ed.
McGraw-Hill, Inc., New York, 1978.

3. Cullen, Christopher Patrick
Design and Evaluation of Weight and Angle Sensors for Gait Training of Above-Knee Amputees
S.M Thesis, MIT Department of Mechanical Engineering, May 1984.

4. Goldfarb, Michael
Control for a Self-contained Microcomputer-controlled Above-knee Prosthesis
S. M. Thesis, Department of Mechanical Engineering, October 25, 1991.

5. Harper, Charles A., Editor-in-chief
Handbook of Plastics, Elastomers, and Composites, 3rd Ed.
McGraw-Hill, New York, 1996.

6. Inman, V., Ralston, H., and Todd, F.
Human Walking
Williams & Wilkins, Baltimore, Maryland, 1981.

7. Pratt, Gill
Mechanism and Control for a Self-Programming Gait Adaptive Knee Prosthesis
MIT Leg Laboratory Research Proposal, 1997.

8. Rothbart, Harold A.
Mechanical Design and Systems Handbook.
McGraw-Hill, New York, 1964.

9. Shurr, D. and Cook, T.
Prosthetics & Orthotics
Appleton & Lange, Norwalk, Connecticut, 1990.

10. Winter, David A. and Sienko, Susan E.
Biomechanics of Below-Knee Amputee Gait
Journal of Biomechanics, Vol. 21, No. 5, pp. 361-367, 1988.

Data Sheets and Suppliers

11. Model 7000: Thin-Film Pressure Sensor Data Sheet
12. Application Notes for Model 7000
Advanced Custom Sensors, Inc.
18 Technology Drive, Suite 139
Irvine, California 92618
(714) 453-8988
http://www.acsensor.com/

13. Model 83 Data Sheet
EG&G IC Sensors
1701 McCarthy Blvd.
Milipitas CA, 95035-7416
1-800 767-1888
http://www.egg-inc.com/

GE Silicones
General Electric Company
260 Hudson River Road
Winterford, New York 12188
1-800 255-8886
http://www.ge.com/silicones/index.html

14. FSR Integration Guide & Evaluation Part Catalog
Interlink Electronics
546 Flynn Road
Camarillo, CA 93012
(805) 484-1331
http://www.interlinkelec.com

15. Honeywell/Micro Switch 40PC Series Data Sheets
Honeywell, Micro Switch Division
11 West Spring Street
Freeport, Illinois 61032
1-800-537-6945
http://www.honeywell.com/sensing/

16. Semiconductor Technical Data sheet MPX5700 Series
17. Semiconductor Technical Data sheet MPX5999 Series
18. Media Isolation Techniques for Motorola MPX Series Pressure Sensors
Motorola SPS
Semiconductor Service Center
3102 North 56th Street
Phoenix, AZ 85018-6606
1-800 521-6274
http://motorola.com/sps/

Appendix A: Motorola Data Sheets

MOTOROLA
SEMICONDUCTOR TECHNICAL DATA

Order this document
by MPX5700/D

senseon

Integrated Silicon Pressure Sensor On-Chip Signal Conditioned, Temperature Compensated and Calibrated

MPX5700 SERIES

INTEGRATED PRESSURE SENSOR
0 to 700 kPa (0 to 101.5 psi)
0.2 to 4.7 V OUTPUT

The MPX5700 series piezoresistive transducer is a state–of–the–art monolithic silicon pressure sensor designed for a wide range of applications, but particularly those employing a microcontroller or microprocessor with A/D inputs. This patented, single element transducer combines advanced micromachining techniques, thin–film metallization, and bipolar processing to provide an accurate, high level analog output signal that is proportional to the applied pressure.

Features

- 2.5% Maximum Error over 0° to 85°C
- Ideally Suited for Microprocessor or Microcontroller–Based Systems
- Available in Differential and Gauge Configurations
- Patented Silicon Shear Stress Strain Gauge
- Durable Epoxy Unibody Element

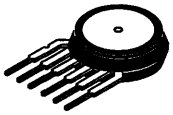

BASIC CHIP CARRIER ELEMENT
CASE 867–08, STYLE 1

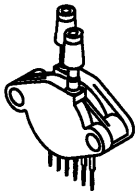

DIFFERENTIAL PORT OPTION
CASE 867C–05, STYLE 1

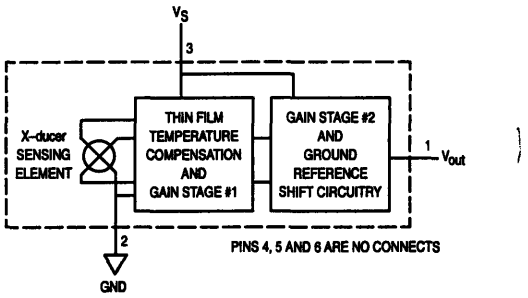

Figure 1. Fully Integrated Pressure Sensor Schematic

PIN NUMBER			
1	V_{out}	4	N/C
2	Gnd	5	N/C
3	V_S	6	N/C

NOTE: *Pins 4, 5, and 6 are internal* device connections. Do not connect to external circuitry or ground. Pin 1 is noted by the notch in the Lead.

MAXIMUM RATINGS(1)

Parametrics	Symbol	Value	Unit
Overpressure (P2 ≤ 1 Atmosphere)	$P1_{max}$	2800	kPa
Burst Pressure (P2 ≤ 1 Atmosphere)	$P1_{burst}$	5000	kPa
Storage Temperature	T_{stg}	−40 to +125	°C
Operating Temperature	T_A	−40 to +125	°C

1. T_C = 25°C unless otherwise noted. Maximum Ratings apply to Case 867–08 only.
2. Extended exposure at the specified limits may cause permanent damage or degradation to the device.
3. This sensor is designed for applications where P1 is always greater than, or equal to P2.

REV 2

MOTOROLA

OPERATING CHARACTERISTICS (V_S = 5.0 Vdc, T_A = 25°C unless otherwise noted, P1 > P2)

Characteristic		Symbol	Min	Typ	Max	Unit
Pressure Range[1]		P_{OP}	0	—	700	kPa
Supply Voltage[2]		V_S	4.75	5.0	5.25	Vdc
Supply Current		I_o	–	7.0	10	mAdc
Zero Pressure Offset[3]	(0 to 85°C)	V_{off}	0.088	0.2	0.313	Vdc
Full Scale Output[4]	(0 to 85°C)	V_{FSO}	4.587	4.7	4.813	Vdc
Full Scale Span[5]	(0 to 85°C)	V_{FSS}	—	4.5	—	Vdc
Accuracy[6]	(0 to 85°C)	—	—	—	± 2.5	$\%V_{FSS}$
Sensitivity		V/P	—	6.4	—	mV/kPa
Response Time[7]		t_R	—	1.0	—	ms
Output Source Current at Full Scale Output		I_{O+}	—	0.1	—	mAdc
Warm–Up Time[8]		—	—	20	—	ms

Decoupling circuit shown in Figure 4 required to meet electrical specifications.

MECHANICAL CHARACTERISTICS

Characteristic	Symbol	Min	Typ	Max	Unit
Weight, Basic Element (Case 867)	—	—	4.0	—	Grams
Cavity Volume	—	—	—	0.01	IN^3
Volumetric Displacement	—	—	—	0.001	IN^3

NOTES:
1. 1.0 kPa (kiloPascal) equals 0.145 psi.
2. Device is ratiometric within this specified excitation range.
3. Offset (V_{off}) is defined as the output voltage at the minimum rated pressure.
4. Full Scale Output (V_{FSO}) is defined as the output voltage at the maximum or full rated pressure.
5. Full Scale Span (V_{FSS}) is defined as the algebraic difference between the output voltage at full rated pressure and the output voltage at the minimum rated pressure.
6. Accuracy (error budget) consists of the following:
   - Linearity: Output deviation from a straight line relationship with pressure over the specified pressure range.
   - Temperature Hysteresis: Output deviation at any temperature within the operating temperature range, after the temperature is cycled to and from the minimum or maximum operating temperature points, with zero differential pressure applied.
   - Pressure Hysteresis: Output deviation at any pressure within the specified range, when this pressure is cycled to and from the minimum or maximum rated pressure, at 25°C.
   - TcSpan: Output deviation over the temperature range of 0° to 85°C, relative to 25°C.
   - TcOffset: Output deviation with minimum rated pressure applied, over the temperature range of 0° to 85°C, relative to 25°C.
   - Variation from Nominal: The variation from nominal values, for Offset or Full Scale Span, as a percent of V_{FSS}, at 25°C.
7. Response Time is defined as the time for the incremental change in the output to go from 10% to 90% of its final value when subjected to a specified step change in pressure.
8. Warm–up is defined as the time required for the device to meet the specified output voltage after the pressure has been stabilized.
9. P2 max is 500 kPa.

ON–CHIP TEMPERATURE COMPENSATION, CALIBRATION AND SIGNAL CONDITIONING

Figure 3 illustrates both the Differential/Gauge and the Absolute Sensing Chip in the basic chip carrier (Case 867). A fluorosilicone gel isolates the die surface and wire bonds from the environment, while allowing the pressure signal to be transmitted to the sensor diaphragm. (For use of the MPX5700D in a high pressure, cyclic application, consult the factory.)

The MPX5700 series pressure sensor operating characteristics, and internal reliability and qualification tests are based on use of dry air as the pressure media. Media, other than dry air, may have adverse effects on sensor performance and long–term reliability. Contact the factory for information regarding media compatibility in your application.

Figure 4 shows a typical decoupling circuit for interfacing the sensor to the A/D input of a microprocessor. Proper decoupling of the power supply is recommended.

Figure 2 shows the sensor output signal relative to pressure input. Typical, minimum, and maximum output curves are shown for operation over a temperature range of 0° to 85°C using the decoupling circuit below. (The output will saturate outside of the specified pressure range.)

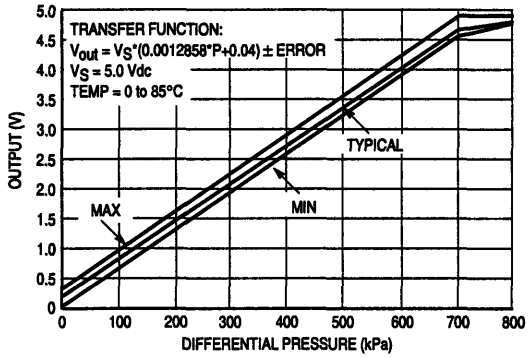

Figure 2. Output versus Pressure Differential

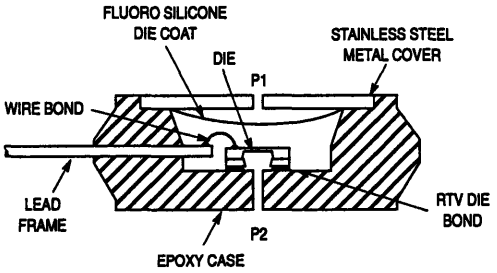

Figure 3. Cross–Sectional Diagram (Not to Scale)

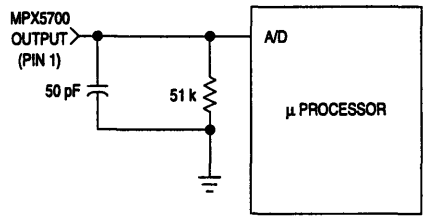

Figure 4. Typical Decoupling Filter for Sensor to Microprocessor Interface

PRESSURE (P1)/VACUUM (P2) SIDE IDENTIFICATION TABLE

Motorola designates the two sides of the pressure sensor as the Pressure (P1) side and the Vacuum (P2) side. The Pressure (P1) side is the side containing fluoro silicone gel which protects the die from harsh media. The Motorola MPX pressure sensor is designed to operate with positive differential pressure applied, P1 > P2.

The Pressure (P1) side may be identified by using the table below:

Part Number	Case Type	Pressure (P1) Side Identifier
MPX5700D	867–08	Stainless Steel Cap
MPX5700DP	867C–05	Side with Part Marking
MPX5700GP	867B–04	Side with Port Attached
MPX5700GS	867E–03	Side with Port Attached
MPX5700GSX	867F–03	Side with Port Attached

ORDERING INFORMATION

The MPX5700 pressure sensor is available in differential and gauge configurations. Devices are available in the basic element package or with pressure port fittings that provide printed circuit board mounting ease and barbed hose pressure connections.

Device Type	Options	Case Type	MPX Series	
			Order Number	Device Marking
Basic Element	Differential	867–08	MPX5700D	MPX5700D
Ported Elements	Differential Dual Ports	867C–05	MPX5700DP	MPX5700DP
	Gauge	867B–04	MPX5700GP	MPX5700GP
	Gauge, Axial	867E–03	MPX5700GS	MPX5700D
	Gauge, Axial PC Mount	867F–03	MPX5700GSX	MPX5700D

PACKAGE DIMENSIONS

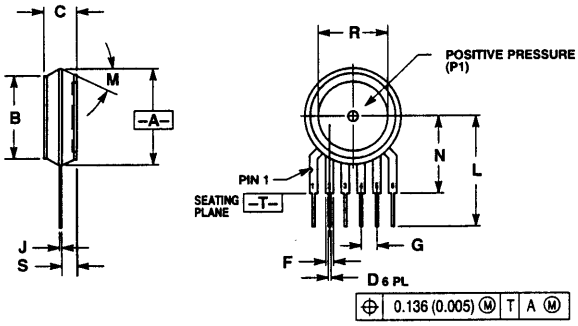

NOTES:
1. DIMENSIONING AND TOLERANCING PER ANSI Y14.5M, 1982.
2. CONTROLLING DIMENSION: INCH.
3. DIMENSION -A- IS INCLUSIVE OF THE MOLD STOP RING. MOLD STOP RING NOT TO EXCEED 16.00 (0.630).

DIM	INCHES		MILLIMETERS	
	MIN	MAX	MIN	MAX
A	0.595	0.630	15.11	16.00
B	0.514	0.534	13.06	13.56
C	0.200	0.220	5.08	5.59
D	0.027	0.033	0.68	0.84
F	0.048	0.064	1.22	1.63
G	0.100 BSC		2.54 BSC	
J	0.014	0.016	0.36	0.40
L	0.695	0.725	17.65	18.42
M	30° NOM		30° NOM	
N	0.475	0.495	12.07	12.57
R	0.430	0.450	10.92	11.43
S	0.090	0.105	2.29	2.66

STYLE 1:
PIN 1. VOUT
2. GROUND
3. VCC
4. V1
5. V2
6. VEX

CASE 867–08
ISSUE N

BASIC ELEMENT (A, D)

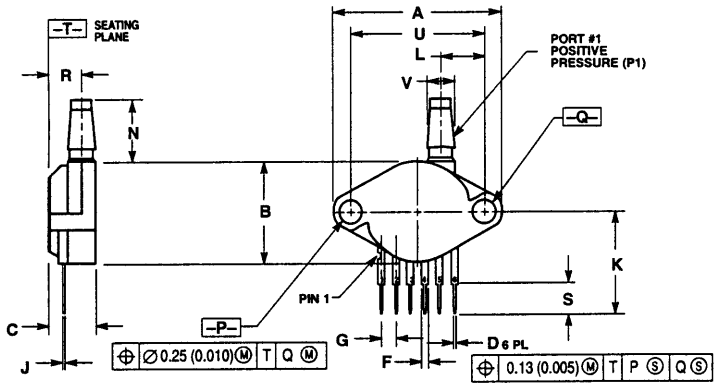

NOTES:
1. DIMENSIONING AND TOLERANCING PER ANSI Y14.5M, 1982.
2. CONTROLLING DIMENSION: INCH.

DIM	INCHES		MILLIMETERS	
	MIN	MAX	MIN	MAX
A	1.145	1.175	29.08	29.85
B	0.685	0.715	17.40	18.16
C	0.305	0.325	7.75	8.26
D	0.027	0.033	0.68	0.84
F	0.048	0.064	1.22	1.63
G	0.100 BSC		2.54 BSC	
J	0.014	0.016	0.36	0.41
K	0.695	0.725	17.65	18.42
L	0.290	0.300	7.37	7.62
N	0.420	0.440	10.67	11.18
P	0.153	0.159	3.89	4.04
Q	0.153	0.159	3.89	4.04
R	0.230	0.250	5.84	6.35
S	0.220	0.240	5.59	6.10
U	0.910 BSC		23.11 BSC	
V	0.182	0.194	4.62	4.93

STYLE 1:
PIN 1. V_{OUT}
2. GROUND
3. V_{CC}
4. V1
5. V2
6. V_{EX}

CASE 867B–04
ISSUE E

PRESSURE SIDE PORTED (AP, GP)

PACKAGE DIMENSIONS–CONTINUED

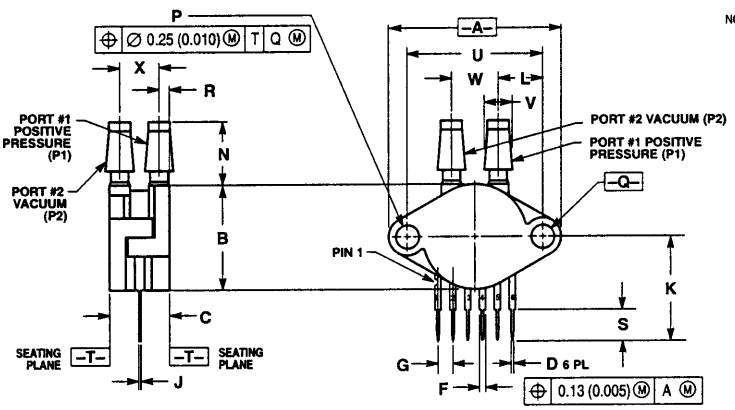

NOTES:
1. DIMENSIONING AND TOLERANCING PER ANSI Y14.5M, 1982.
2. CONTROLLING DIMENSION: INCH.

	INCHES		MILLIMETERS	
DIM	MIN	MAX	MIN	MAX
A	1.145	1.175	29.08	29.85
B	0.685	0.715	17.40	18.16
C	0.405	0.435	10.29	11.05
D	0.027	0.033	0.68	0.84
F	0.048	0.064	1.22	1.63
G	0.100 BSC		2.54 BSC	
J	0.014	0.016	0.36	0.41
K	0.695	0.725	17.65	18.42
L	0.290	0.300	7.37	7.62
N	0.420	0.440	10.67	11.18
P	0.153	0.159	3.89	4.04
Q	0.153	0.159	3.89	4.04
R	0.063	0.083	1.60	2.11
S	0.220	0.240	5.59	6.10
U	0.910 BSC		23.11 BSC	
V	0.182	0.194	4.62	4.93
W	0.310	0.330	7.87	8.38
X	0.248	0.278	6.30	7.06

STYLE 1:
PIN 1. V_{OUT}
2. GROUND
3. V_{CC}
4. V1
5. V2
6. V_{EX}

CASE 867C–05
ISSUE F

PRESSURE AND VACUUM SIDES PORTED (DP)

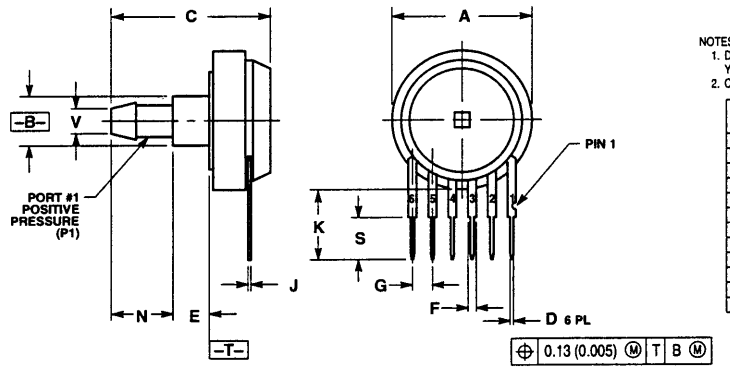

NOTES:
1. DIMENSIONING AND TOLERANCING PER ANSI Y14.5M, 1982.
2. CONTROLLING DIMENSION: INCH.

	INCHES		MILLIMETERS	
DIM	MIN	MAX	MIN	MAX
A	0.690	0.720	17.53	18.28
B	0.245	0.255	6.22	6.48
C	0.780	0.820	19.81	20.82
D	0.027	0.033	0.69	0.84
E	0.178	0.186	4.52	4.72
F	0.048	0.064	1.22	1.63
G	0.100 BSC		2.54 BSC	
J	0.014	0.016	0.36	0.41
K	0.345	0.375	8.76	9.53
N	0.300	0.310	7.62	7.87
S	0.220	0.240	5.59	6.10
V	0.182	0.194	4.62	4.93

STYLE 1:
PIN 1. V_{OUT}
2. GROUND
3. V_{CC}
4. V1
5. V2
6. V_{EX}

CASE 867E–03
ISSUE D

PRESSURE SIDE PORTED (AS, GS)

Honeywell

Pressure Sensors

Miniature Signal Conditioned

40PC Series

FEATURES
- Smallest amplified sensor package
- Minimal PCB space
- Fully signal conditioned
- Operating temperature range from -45 to +125°C
- Silicon piezoresistive technology
- Monolithic design
- 6 pin DIP package
- Port designed for O-ring interface
- Excellent media compatibility

TYPICAL APPLICATIONS
- Hospital beds
- Respirators and ventilators
- Oxygen concentrators
- Laboratory equipment
- Nebulizers
- Blood pressure measurement
- Electronic brake systems
- Engine oil level
- Transmission fluid level
- Air conditioning system
- Fuel injection systems

⚠ WARNING
PERSONAL INJURY
- DO NOT USE these products as safety or emergency stop devices, or in any other application where failure of the product could result in personal injury.

Failure to comply with these instructions could result in death or serious injury.

ESD SENSITIVITY: CLASS I

The new cost-effective 40PC Series miniature pressure sensor is the smallest amplified pressure sensor ever introduced by Honeywell's MICRO SWITCH Division. The fully calibrated and temperature-compensated sensor is one of the most robust, covering the widest temperature extremes of Honeywell's pressure products. Additionally, the 40PC Series is compatible with a broad array of media, from dry air and water to refrigerant coolants and engine fuel.

40PC Series miniature pressure sensors provide an analog amplified output. The sensor utilizes a monolithic design based on piezoresistive technology. The components which provide temperature compensation and output amplification are located on the silicon piezoresistive chip.

The sensors operate on a 5 VDC supply voltage and have a 4 VDC span. The output voltage ranges from 0.5 to 4.5 VDC and is linearly proportional to the input pressure. Accuracy at room temperature is 0.2%.

The 6 pin DIP package is designed for convenient printed circuit board mounting. Three pins on one side are active - supply voltage, output voltage and ground. The three pins on the other side can be clipped off for printed circuit board designs which require the sensor's port to be mounted parallel to the board.

⚠ WARNING
MISUSE OF DOCUMENTATION
- The information presented in this product sheet is for reference only. DO NOT USE this document as product installation information.
- Complete installation, operation and maintenance information is provided in the instructions supplied with each product.

Failure to comply with these instructions could result in death or serious injury.

Pressure Sensors

Miniature Signal Conditioned

40PC Series

PERFORMANCE CHARACTERISTICS

Pressure Range		-50 to +50 mmHg
		0 to 15 psi
		0 to 100 psi
		0 to 150 psi
		0 to 250 psi
Overpressure, max.	50 mmHg	±170 mmHg max.
	0 to 15 psi	45 psi
	0 to 100 psi	200 psi
	0 to 150 psi	300 psi
	0 to 250 psi	500 psi
Supply Voltage	All	5 VDC
Supply Current	All	10 mA max.
Output Source Current	All	0.5 mA max.
Output Sink Current	All	1.0 mA max.
Operating Temperature	All	-45 to +125°C (-49 to +257°F)
Storage Temperature	All	-55 to +125°C (-67 to +257°F)
Media Compatibility	Limited to those media which will not attack invar, copper, silicon, stainless steel, glass and solder	

OUTPUT PERFORMANCE @ 25°C, 5 VDC (unless otherwise noted)

Null	50 mmHg	2.50 ± 0.05 VDC
	0 to 15 psi	0.50 ± 0.11 VDC
	0 to 100 psi	0.50 ± 0.04 VDC
	0 to 150 psi	0.50 ± 0.04 VDC
	0 to 250 psi	0.50 ± 0.04 VDC
Full Scale	+50 mmHg	4.50 ± 0.12 VDC
	-50 mmHg	0.50 VDC Typ.
	All others	4.50 VDC Typ.
Span	±50 mmHg	4.00 VDC Typ.
	0 to 15 psi	4.00 ± 0.11 VDC
	0 to 100 psi	4.00 ± 0.09 VDC
	0 to 150 psi	4.00 ± 0.07 VDC
	0 to 250 psi	4.00 ± 0.07 VDC
Sensitivity	±50 mmHg	40.0 mV/mmHg Typ.
	0 to 15 psi	266.6 mV/psi Typ.
	0 to 100 psi	40.0 mV/psi Typ.
	0 to 150 psi	26.6 mV/psi Typ
	0 to 250 psi	16.0 mV/psi Typ
Hysteresis & Repeatability	All	0.15% Span, Typ.

Pressure Sensors

Miniature Signal Conditioned

40PC Series

ELECTRICAL CONNECTION

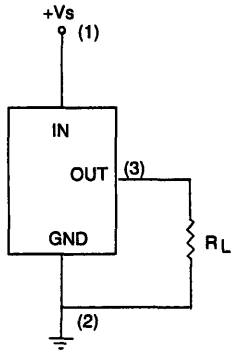

NOTES:

1. Square corner marks pin 1 (Vs).
2. Output can be shorted to ground. Do not short to the positive supply voltage.

MOUNTING DIMENSIONS (for reference only)

mm

In.

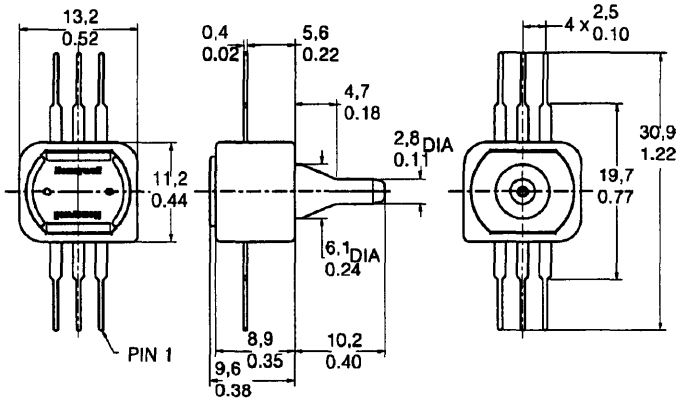

ORDER GUIDE

40PC □□□ □ □ □

Port Style
A Straight

Lead Style
1 Unformed
2 Formed away from port
3 Formed towards port

Pressure Type
G Gage

Pressure Range
001 ± 50 mmHg
015 0 to 15 psi
100 0 to 100 psi
150 0 to 150 psi
250 0 to 250 psi

WARRANTY/REMEDY

Honeywell warrants goods of its manufacture as being free of defective materials and faulty workmanship. Contact your local sales office for warranty information. If warranted goods are returned to Honeywell during the period of coverage, Honeywell will repair or replace without charge those items it finds defective. The foregoing is Buyer's sole remedy and is **in lieu of all other warranties, expressed or implied, including those of merchantability and fitness for a particular purpose.**

For application assistance, current specifications, pricing or name of the nearest Authorized Distributor, contact a nearby sales office. Or call:

1-800-537-6945 USA
1-800-737-3360 Canada
1-815-235-6847 International
FAX
1-815-235-6545 USA
INTERNET
http://www.honeywell.com/sensing/
info@micro.honeywell.com

Specifications may change without notice. The information we supply is believed to be accurate and reliable as of this printing. However, we assume no responsibility for its use.

While we provide application assistance, personally and through our literature, it is up to the customer to determine the suitability of the product in the application.

Honeywell

Helping You Control Your World

MICRO SWITCH
Honeywell Inc.
11 West Spring Street
Freeport, Illinois 61032

Printed with Soy Ink on 50% Recycled Paper

008034-1-EN IL50 GLO 198 Printed in USA

Appendix C: EG&G Model 83 Data Sheets

OEM High Pressure Sensor Sealed Gage and Absolute Stainless Steel Diaphragm 100 mV Output Span

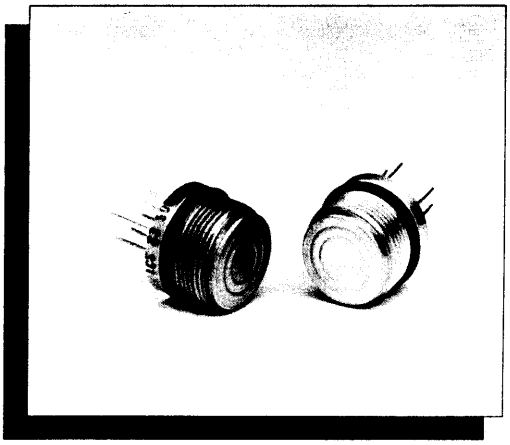

Features

- 316SS All Welded Construction
- Solid State Reliability
- Flush Diaphragm
- Ratiometric
- ± 0.5% Accuracy
- Low Noise
- Infinite Resolution
- Low Cost
- Serialized

Typical Applications

- Pressure Transmitters
- Hydraulic Servo Controls
- Smart Valves
- Tank Levels
- Machine Tools
- Refrigeration
- Air Conditioning
- Food Processing

Standard Ranges

0 to 300 psis	0 to 300 psia
0 to 500 psis	0 to 500 psia
0 to 1000 psis	0 to 1000 psia
0 to 3000 psis	0 to 3000 psia
0 to 5000 psis	0 to 5000 psia

Description

The Models 80 and 83 are media compatible, solid state pressure sensors that are intended for use in high pressure OEM applications where long term stability must be combined with low cost.

The Iso-Pressure 316 stainless steel housing structure utilizes an oil column to couple a diffused, piezoresistive sensor to a convoluted, flush 316 stainless steel diaphragm that can be interfaced with most harsh media.

For the Model 80, temperature compensation and calibration is accomplished with 3 external resistors. The resistor values are included with each sensor. The Model 83 includes an optional ceramic compensation board with these resistors trimmed to the appropriate values.

These pressure sensors are available in both sealed gage and absolute pressure versions from 0-300 psi to 0-5000 psi. Each sensor is individually serialized.

Dimensions

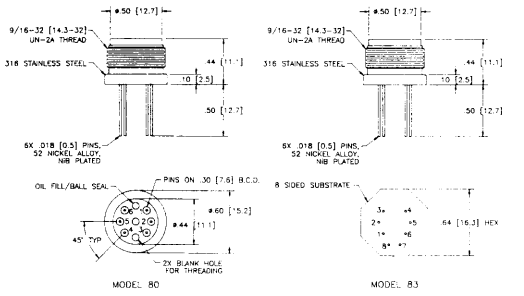

ALL DIMENSIONS ARE IN INCHES (METRIC)

Models 80 and 83

Performance Specifcations

Supply Current = 1.5mA & Ambient Temperature = 25°C (Unless otherwise specified)

PARAMETER	Models 80 and 83			UNITS	NOTES
	MIN	TYP	MAX		
Full-Scale Output Span	50	100	200	mV	
Zero Pressure Output			5	±mV	2,3,4
Static Accuracy			0.5	±%Span	5
Input & Output Resistance	4000	4500	6000	Ω	
Temperature Coefficient - Span			1.0	±% Span	1,2,3
Temperature Coefficient - Zero			1.0	±% Span	1,2,3
Supply Current		1.5	2.0	mA	6
Output Load Resistance	2			MΩ	7
Insulation Resistance (50 VDC)	50			MΩ	
Pressure Overload			3X	Rated	8
Operating Temperature	-20°C to +85°C				
Storage Temperature	-40°C to +125°C				
Media	Compatible with 316 Stainless Steel				
Weight	12 grams				

Notes

1. Temperature Range: 0-50°C in reference to 25°C.
2. For Model 80, with external resistors (R_1 or R_2), (R_3 or R_4) and R_5 included in circuit in Figure 1. If R_1 is required then R_2 is left open ($R_2 = \infty$) and vice versa. If R_3 is required then R_4 is a short ($R_4 = 0$) and vice versa. See Application Note TN-002.
3. A computer printout is supplied with each sensor detailing the values of the 3 required external resistors along with open and short information for the other two locations. For Model 83, a thick film ceramic substrate is provided that contains the specific external resistors, trimmed to the correct value for compensation, and fits directly over the 6 electrical pins for customer soldering. Two additional pins can be connected by the user to the ceramic substrate for use of the gain set resistor.
4. Measured at vacuum for absolute (A) and one standard atmosphere for sealed gage (S).
5. Includes repeatability, pressure hysteresis and linearity (best fit straight line).
6. Guarantees output/input ratiometricity.
7. Prevents increase of TC-Span due to output loading.
8. 3X or 7,500 psi maximum, whichever is less.
9. See Models 81, 84, 151 or 154 for low pressure requirements.
10. Case is threaded (9/16-32).

Ordering Information

80 - 300 - S

- S — Type (S=Sealed Gage, A=Absolute)
- 300 — psi Range
- 80 — Model 80 or 83 (see note 4)

Connections

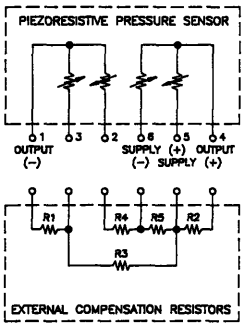

MODEL 80

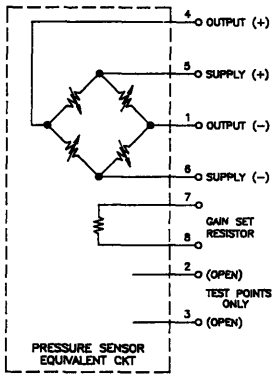

MODEL 83

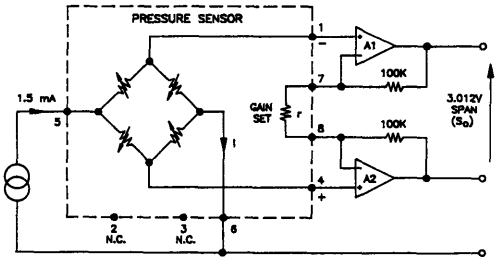

FIGURE 1

IC SENSORS 1701 McCarthy Blvd. Milpitas, California 95035-7416 Fax (408) 432-7322 Phone (408) 432-1800

Appendix D: ACSI Sensor Data Sheets and Amplifier circuit diagrams from Model 7000 application notes

Model 7000 : Thin-Film Pressure Sensor

Features:

- Low Cost
- Excellent static accuracy of ±0.25%
- Stainless steel construction for harsh environments applications
- Custom designs for high volume OEM applications

Description:

The Model 7000 sensor is developed for use in hydraulic, fluid power, exercise equipment, mining equipment and medical equipment. It consists of a metal diaphragm element and a vacuum deposited strain gage. The thin-film technology and advanced manufacturing techniques are incorporated to produce the superior price/performance ratio.

This sensor can be easily modified to meet your mechanical and electrical interface requirements. Other applications include HVAC, industrial/commercial equipment and off-road vehicles. ACSI will perform the custom design to meet the accurate pressure requirement in your OEM applications.

Electrical:

Excitation Voltage (Vdc or Vac,rms):	10.0 nominal, 15.0 maximum
Input Resistance(Ohm):	5000±2000
Output Resistance(Ohm):	5000±2000
Insulation Resistance(Mohm):	1000 @ 50 Vdc
Bridge Configuration:	Full Wheatstone Bridge
Electrical Connection:	6" of Four 30 AWG Unshielded Lead Wires

Sensor Operating Characteristics:

Dash Number	-1	-2	-3	-4	-5	-6
Range (psig)	0-100	0-200	0-500	0-1000	0-3000	0-5000
Full Scale Output (mV/V)	2.0±0.2	2.0±0.2	2.0±0.2	2.0±0.2	2.0±0.2	2.0±0.2
Zero(%FS)[1]	±10	±10	±10	±10	±10	±10
Static Error Band(%FS)[2]	0.25	0.25	0.25	0.25	0.25	0.25
Warm Up Time (Sec)	1	1	1	1	1	1
Stability (% FS/yr)	±0.2	±0.2	±0.2	±0.2	±0.2	±0.2

Environmental Effects:

Seal	Urethane Coated
Compensated Temperature Range	30 °F TO +180 °F(-18 °C TO +82 °C)

Operating Temperature Range[3]	-65 °F TO +300 °F(-54 °C TO +149 °C)					
Temperature Effect on						
Zero Balance (%FS/°F)	±0.02	±0.02	±0.02	±0.02	±0.02	±0.02
Full Scale (%FS/°F)	±0.02	±0.02	±0.02	±0.02	±0.02	±0.02
Overpressure Zero Shfit(%FS)	±0.25	±0.25	±0.25	±0.25	±0.25	±0.25 Overpressure
Range (psi) 200	400	1000	2000	6000	10000	
Burst Pressure (psi)	300	600	1500	3000	9000	15000

Mechanical:

Material	Stainless Steel

NOTE: 1. Zero Balance may change with installation.
2. Static error band is the RSS of nonlinearity, hysteresis and repeatability.
3. Higher operating temperature available on special order.

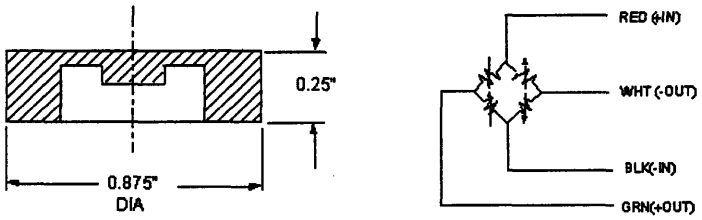

Back To Home Page | Price List | Thin-Film Sensors| Micromachined Silicon Sensors | Electronic Modules| Gauging Service| Micromachining Service | Contact ACSI

longer meet this requirement. They have been replaced by low-cost sensors using strain-gaged pressure diaphragms.

In many situations the coating fluid is passed through filters prior to being sprayed. This will remove whatever particulate matter is picked up as the liquid is being sprayed and re-circulated. Measuring the pressure drops across the filter serves to indicate the condition of the filter.

5. COMPRESSOR MONITORING

In normal operation compressors can be expected to function with all of their operating parameters falling within normal limits. In terms of pressure these parameters could include inlet and discharge, used air and water, and the drop across both air and oil filters.

If any pressure falls outside of the normal values, the operator will be alerted that some correction is needed. The Model 7000 can be used for all pressure measurement. They are mounted in the control box and connected to the pressure sources through tubing. Electrical connections are to an adjacent microprocessor. These sensors offer small size and stainless diaphragm. Its close proximity to the microprocessor allows the use of its low level signals without any amplification. The price of the sensor permits the manufacturers to offer a cost effective and totally integrated diagnostic system.

6. MEDICAL EQUIPMENT

In sterilization chamber, pressure sensor is used to measure the pressure of saturated steam at 170 °C. The chamber operates continuously. Stability and repeatability are critical to this application. The Model 7000 is a perfect fit for this application. Its thin-film gages can operate above 170 °C continuously and also offers the extreme long-term stability.

SIGNAL-CONDITIONING CIRCUITS:

1. BRIDGE AMPLIFIERS

Strain gage sensors require high input impedance amplifiers to avoid performance degradation. The bridge impedance changes with temperature, when a low input impedance differential amplifier is used, leading to a temperature dependent gain non-linearity. Designs for three suitable bridge amplifiers are shown below.

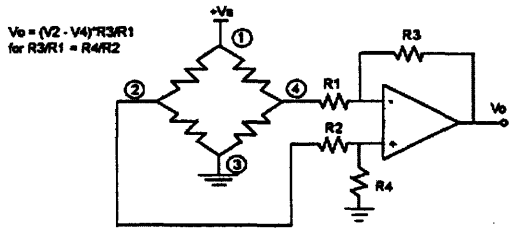

Figure 13.

Figure 13 illustrates a circuit using only one amplifier. An amplifier with a low TC of input offset current, such as M108, is required to permit use of large value input resistors (such as 100K) to minimize bridge loading. The disadvantage of this method is that two resistors must be adjusted to change gain.

Next Back to the Thin Film Sensors Back to the Homepage

Figure 14 illustrates a circuit using two amplifiers. Two resistors must also be adjusted to change gain in this circuit. It has an inherently high input impedance.

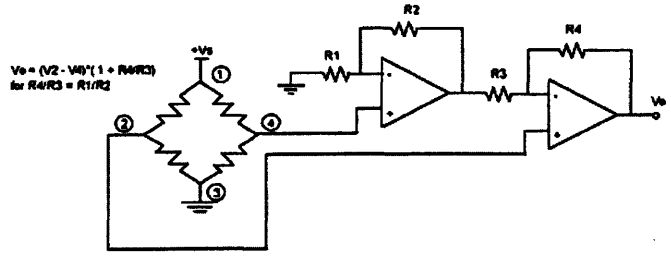

Figure 14.

The circuit in Figure 15 requires four operational amplifiers, but allows gain to be changed with a single resistor. The first stage inherently has a common mode gain of unity. Thus, this circuit can be made significantly less sensitive to common mode errors due to resistor mismatch by placing all of the gain in the first stage and using the output stage as a unity gain summing amplifier. This circuit also has an inherently high input impedance.

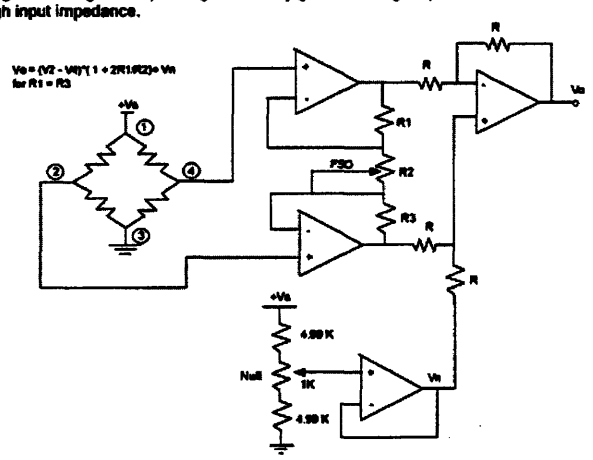

Figure 15.

In amplified voltage circuit, the output is typically set to an industry-standard output range: 1 V to 5 V. The one volt offset voltage is deliberate because the amplifier output can not go down to zero volt. Making 'zero' output equal to one volt allows precise adjustment. The full scale is set at five volt in order to work with digital circuitry.

Appendix E: Interlink Electronics FSR Data Sheets

Force Sensing Resistors
An Overview of the Technology

Force Sensing Resistors (FSR) are a polymer thick film (PTF) device which exhibits a decrease in resistance with an increase in the force applied to the active surface. Its force sensitivity is optimized for use in human touch control of electronic devices. FSRs are not a load cell or strain gauge, though they have similar properties. FSRs are not suitable for precision measurements.

FSR Construction

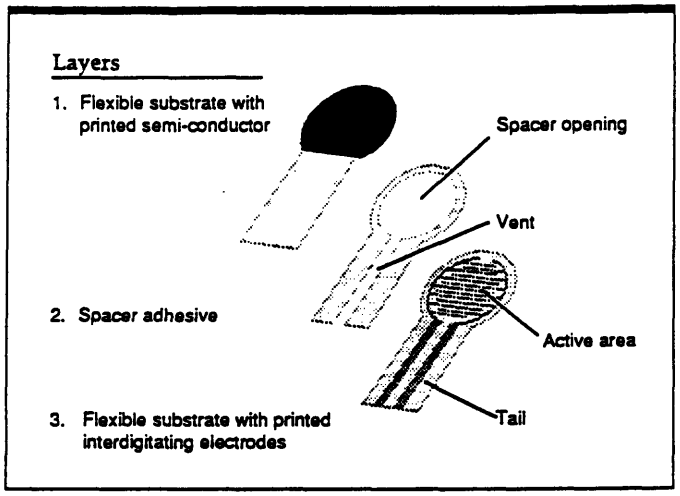

Force vs. Resistance

The force vs. resistance characteristic shown in Figure 1 provides an overview of FSR typical response behavior. For interpretational convenience, the force vs. resistance data are plotted on a log/log format. These data are representative of our typical devices, with this particular force-resistance characteristic being the response of evaluation part #402 (0.5" [12.7 mm] diameter circular active area). A stainless steel actuator with a 0.4" [10.0 mm] diameter hemispherical tip of 60 durometer polyurethane rubber was used to actuate the FSR device. In general, FSR response approximately follows an inverse power-law characteristic (roughly 1/R).

Referring to Figure 1, at the low force end of the force-resistance characteristic, a switch-like response is evident. This turn-on threshold, or "break force", that swings the resistance from greater than 100 kΩ to about 10 kΩ (the beginning of the dynamic range that follows a power-law) is determined by the substrate and overlay thickness and flexibility, size and shape of the actuator, and spacer-adhesive thickness (the gap between the facing conductive elements). Break force increases with increasing substrate and overlay rigidity, actuator size, and spacer-adhesive thickness. Eliminating the adhesive, or keeping it well away from the area where the force is being applied, such as the center of a large FSR device, will give it a lower rest resistance (e.g. stand-off resistance). Any pre-loading of a FSR will also yield the same result.

Force vs. Resistance

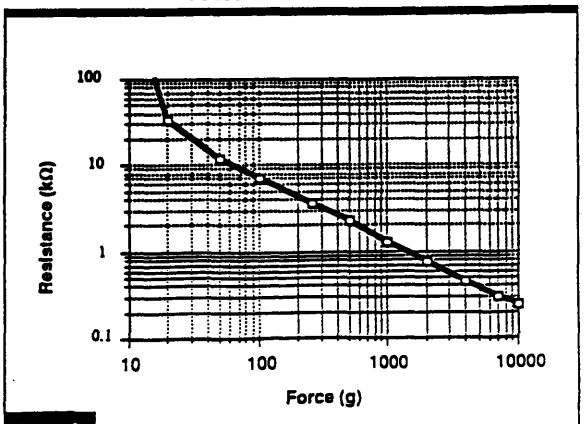

Figure 1

At the high force end of the dynamic range, the response deviates from the power-law behavior, and eventually saturates to a point where increases in force yield little or no decrease in resistance. Under the test conditions of Figure 1, this saturation force is beyond 10 kg. The saturation point is more a function of pressure than force. The saturation pressure of a typical FSR is on the order of 100 to 200 psi. For the data shown in Figures 1, 2 and 3, the actual measured pressure range is 0 to 175 psi (0 to 22 lbs applied over 0.125 in^2). Forces higher than the saturation force can be measured by spreading the force over a greater area; the overall pressure is then kept below the saturation point, and dynamic response is maintained. However, the converse of this effect is also true, smaller actuators will saturate FSRs earlier in the dynamic range, since the saturation point is reached at a lower force.

Force vs. Conductance (0-10 Kg)

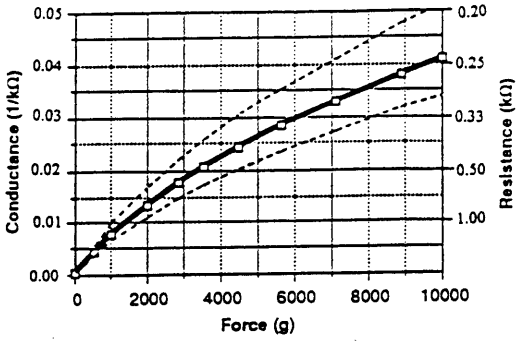

Figure 2

Force vs. Conductance (0-1 Kg) Low Force Range

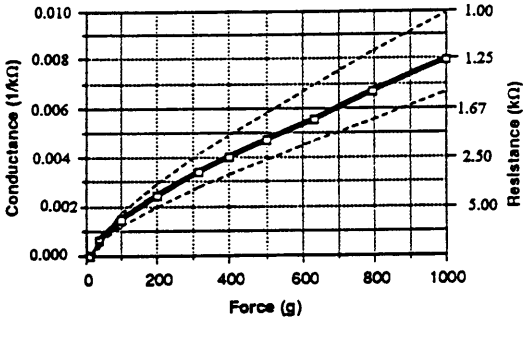

Figure 3

Force vs. Conductance

In Figure 2, the force is plotted vs. conductance (the inverse of resistance: 1/R). This format allows interpretation on a linear scale. For reference, the corresponding resistance values are also included on the right vertical axis. A simple circuit called a current-to-voltage converter (see page 20) gives a voltage output directly proportional to FSR conductance and can be useful where response linearity is desired. Figure 2 also includes a typical part-to-part repeatability envelope. This error band determines the maximum accuracy of any general force measurement. The spread or width of the band is strongly dependent on the repeatability of any actuating and measuring system, as well as the repeatability tolerance held by Interlink Electronics during FSR production. Typically, the part-to-part repeatability tolerance held during manufacturing ranges from ± 15% to ± 25% of an established nominal resistance.

Figure 3 highlights the 0-1 kg (0-2.2 lbs) range of the force-conductance characteristic. As in Figure 2, the corresponding resistance values are included for reference. This range is common to human interface applications. Since the conductance response in this range is fairly linear, the force resolution will be uniform and data interpretation simplified. The typical part-to-part error band is also shown for this touch range. In most human touch control applications this error is insignificant, since human touch is fairly inaccurate. Human factors studies have shown that in this force range repeatability errors of less than ± 50% are difficult to discern by touch alone.

Evaluation Parts
Descriptions and Dimensions

Part #400 (0.2" Circle)

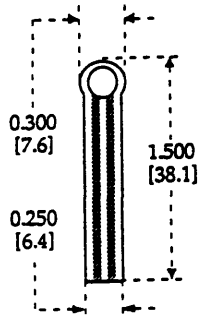

Active Area 0.2"[5.0] diameter

Nominal Thickness 0.012 [0.30]

Material Build:

Semiconductive Layer
0.004" [0.10] PES

Spacer Adhesive
0.002"[0.05] Acrylic

Conductive Layer
0.004" [0.10] PES

Rear Adhesive
0.002"[0.05] Acrylic

Connectors
Solder Tabs (Not Shown)

Dimensions in brackets: millimeters. Dimensional Tolerance: ± 0.015" [0.4]. Thickness Tolerance: ± 10%

Part #402 (1/2" Circle)

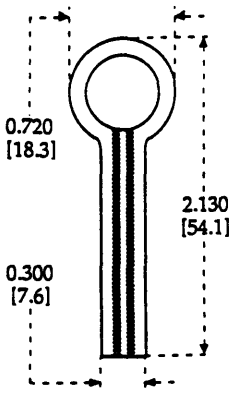

Active Area 0.5"[12.7] diameter

Nominal Thickness 0.018 [0.46]

Material Build:

Semiconductive Layer
0.005" [0.13] Ultem

Spacer Adhesive
0.006"[0.15] Acrylic

Conductive Layer
0.005" [0.13] Ultem

Rear Adhesive
0.002"[0.05] Acrylic

Connectors
Solder Tabs (Not Shown)

Part #406 (1-1/2" Square)

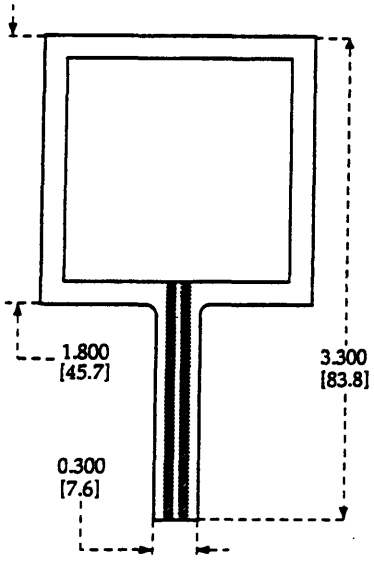

Active Area 1.5"[38.1] x 1.5"[38.1]

Nominal Thickness 0.018 [0.46]

Material Build:

Semiconductive Layer
0.005" [0.13] Ultem

Spacer Adhesive
0.006"[0.15] Acrylic

Conductive Layer
0.005" [0.13] Ultem

Rear Adhesive
0.002"[0.05] Acrylic

Connectors
Solder Tabs (Not Shown)

Dimensions in brackets: millimeters. Dimensional Tolerance: ± 0.015" [0.4]. Thickness Tolerance: ± 10%

General FSR Characteristics

These are typical parameters. The FSR is a custom device and can be made for use outside these characteristics. Consult Sales Engineering with your specific requirements.

Simple FSR Devices and Arrays

Parameter	Value	Notes
Size Range	Max = 20" x 24" (51 x 61 cm) Min = 0.2" x 0.2" (0.5 x 0.5 cm)	Any shape
Device Thickness	0.008" to 0.050" (0.20 to 1.25 mm)	Dependent on materials
Force Sensitivity Range	< 100 g to > 10 kg	Dependent on mechanics
Pressure Sensitivity Range	< 1.5 psi to > 150 psi (< 0.1 kg/cm² to > 10 kg/cm²)	Dependent on mechanics
Part-to-Part Force Repeatability	± 15% to ± 25% of established nominal resistance	With a repeatable actuation system
Single Part Force Repeatability	± 2% to ± 5% of established nominal resistance	With a repeatable actuation system
Force Resolution	Better than 0.5% full scale	
Break Force (Turn-on Force)	20 g to 100 g (0.7 oz to 3.5 oz)	Dependent on mechanics and FSR build
Stand-Off Resistance	> 1 MΩ	Unloaded, unbent
Switch Characteristic	Essentially zero travel	
Device Rise Time	1–2 msec (mechanical)	
Lifetime	> 10 million actuations	
Temperature Range	-30°C to +170°C	Dependent on materials
Maximum Current	1 mA/cm² of applied force	
Sensitivity to Noise/Vibration	Not significantly affected	
EMI/ESD	Passive device	
Lead Attachment	Standard flex circuit techniques	

For Linear Pots

Parameter	Value	Notes
Positional Resolution	0.003" to 0.02" (0.075 to 0.5 mm)	Dependent on actuator size
Positional Accuracy	better than ± 1% of full length	

FSR terminology is defined on pages 13 and 14 of this guide.

Appendix F: CAD drawings of final sensor design

Outer cylinder

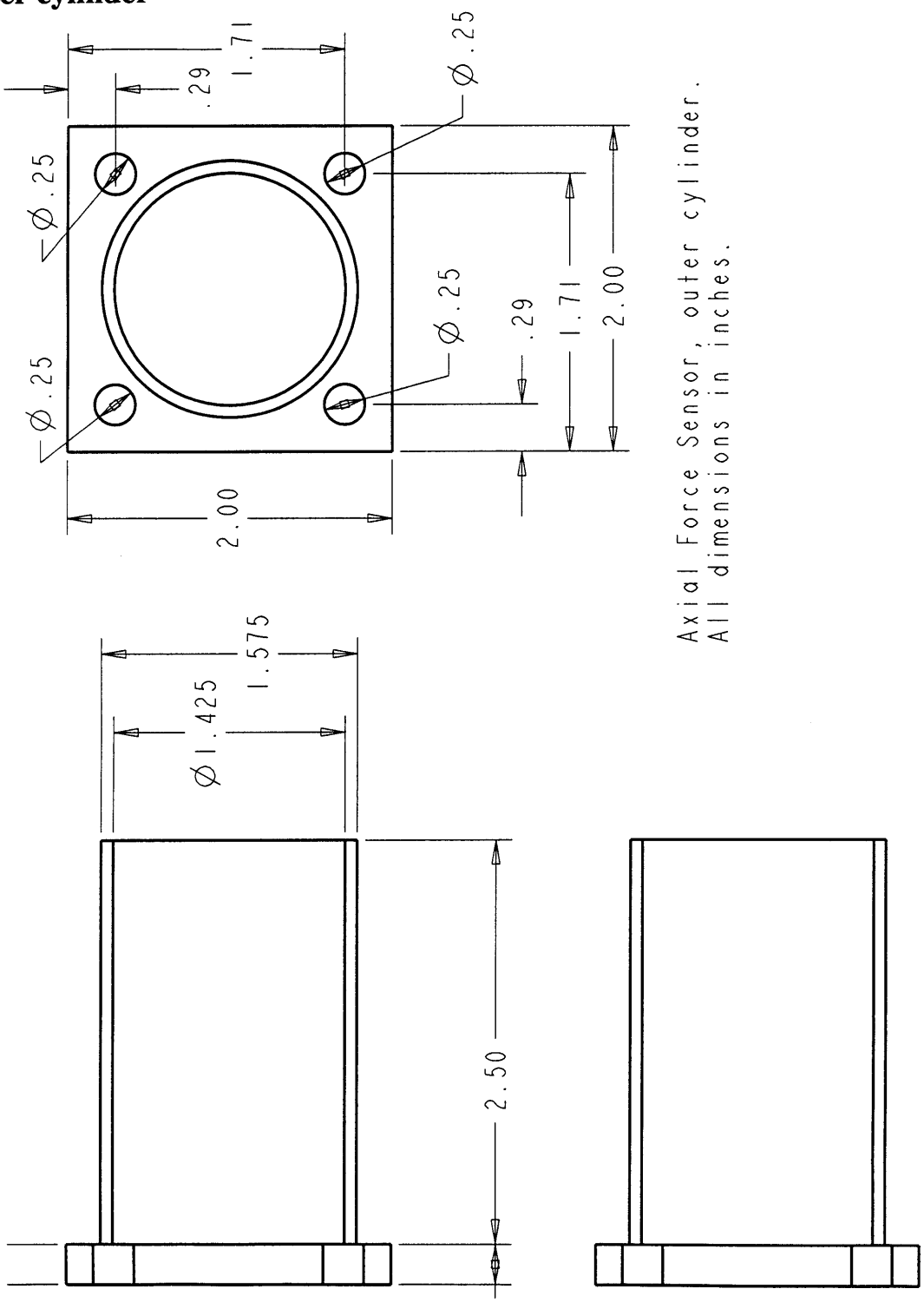

Inner Cylinder